ACS OMEGA

Open Access

http://pubs.acs.org/journal/acsodf

Article

Topical Application of Baicalin Combined with Echinacoside Ameliorates Psoriatic Skin Lesions by Suppressing the Inflammation-Related TNF Signaling Pathway and the Angiogenesis-Related VEGF Signaling Pathway

Yi Chen, Yongfang Wang, Shasha Song, Xiaoli Zhang, Lili Wu, Jianbing Wu, and Xinyu Li*

Cite This: *ACS Omega* 2023, 8, 40260−40276

Read Online

ACCESS | Metrics & More | Article Recommendations | Supporting Information

ABSTRACT: Baicalin (BAI), the main active component of *Scutellaria baicalensis*, has significant anti-inflammatory and antibacterial effects. Echinacoside (ECH), an active component from *Echinacea purpurea*, has significant antiangiogenesis and antioxidant effects. In previous studies, BAI or ECH has been used for some skin inflammation problems by topical treatment. Psoriasis (PSO) is a common inflammatory skin disease with typical features such as excessive inflammatory response and vascular proliferation in skin lesions. Because of the anti-inflammatory effect of BAI and the antiangiogenic activity of ECH, it is proposed that the combination of BAI and ECH can ameliorate psoriatic skin lesions better than a single component. This study aims to explore the effects and potential mechanisms of BAI combined with ECH on imiquimod (IMQ)-induced psoriatic skin lesions by topical treatment. Transcriptome analysis first showed that the TNF signaling pathway and the VEGF signaling pathway were significantly enriched in IMQ-induced psoriatic skin lesions. Topical application of BAI combined with ECH could ameliorate IMQ-induced skin lesions in mice, especially the better effects of B2-E1 (BAI/ECH = 2:1). Network pharmacology analysis and molecular docking indicated that BAI-treated PSO on the skin by regulating the TNF signaling pathway, and ECH treated PSO on the skin by regulating the VEGF signaling pathway. Meanwhile, the ELISA test and the qPCR assay showed that BAI combined with ECH could inhibit the expression of key cytokines and genes related to the TNF signaling pathway and the VEGF signaling pathway. Zebrafish experiments demonstrated the anti-inflammatory and antiangiogenic effects of BAI combined with ECH and revealed the potential mechanisms associated with regulating the inflammation-related TNF signaling pathway and the angiogenesis-related VEGF signaling pathway. This suggested that BAI combined with ECH may be a promising topical agent to ameliorate psoriatic skin lesions in the future.

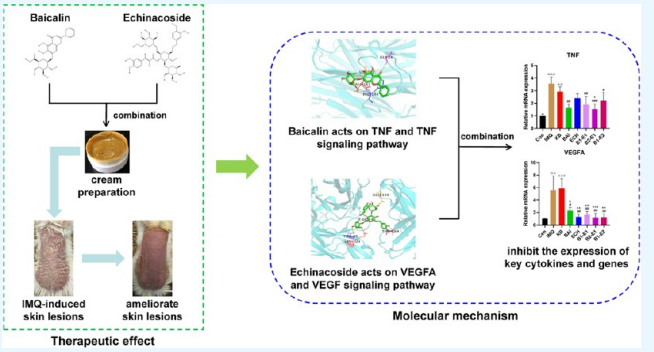

1. INTRODUCTION

Psoriasis (PSO) is a complex chronic inflammatory skin disease with typical pathological features including hyperproliferation of epidermal keratinocytes, dermal microvascular hyperplasia, and intradermal inflammatory cell infiltration.[1,2] It presents psoriatic skin lesions such as erythema, scales, and epidermal thickening in clinic.[3] According to the statistics, approximately 2% of the population worldwide has been affected by PSO.[4] Thus, it is urgent to search for effective drugs to treat PSO.

For the symptoms of skin lesions in PSO, it is necessary to adopt topical drug therapies. In clinical practice, topical application of retinoids, vitamin D3 analogues (calcipotriol, tacalcitol), and glucocorticoids (halometasone, clobetasol propionate) can effectively alleviate psoriatic skin lesions. However, the inherent side effects of these drugs such as skin irritation and limitation of medication time also exist.[5] It has been reported that long-term use of glucocorticoids will also cause skin atrophy, telangiectasia, and other problems.[6] Therefore, it is important to develop potential topical drugs with reduced toxicity and positive therapeutic efficacy. In recent years, herbal medicinal products with relatively low toxicity and fewer side effects have attracted more and more concern. They are suitable for long-term use, especially in the treatment of chronic inflammatory diseases such as PSO.[7]

Baicalin (BAI) is the main active component of *Scutellaria baicalensis*, which has multiple pharmacological effects such as

Received: June 15, 2023
Accepted: September 28, 2023
Published: October 16, 2023

anti-inflammatory effect, neuroprotection, antitumor effect, and liver protection.[8−11] Many studies have further shown the therapeutic potential of BAI on skin diseases by topical treatment. For example, topical application of BAI showed therapeutical effects on pressure ulcers, skin inflammation, and hair loss.[12−14] Echinacoside (ECH), a major bioactive compound of *Echinacea purpurea*, has shown multiple effects such as antiangiogenic activity, antioxidant activity, anti-inflammatory effect, and antitumor effect.[15−19] Particularly, ECH exhibits significant potential in treating skin diseases such as UVB irradiation-induced skin damage by topical treatment.[20] In summary, BAI and ECH could be promising agents in the treatment of inflammatory skin diseases. Because of the significant anti-inflammatory effect of BAI and the obvious antiangiogenic activity of ECH, it was further proposed that the combination of BAI and ECH could better ameliorate the psoriatic skin lesions with typical pathological features including excessive inflammation and abnormal angiogenesis. Therefore, this study was then performed to explore the therapeutic potential of BAI combined with ECH for psoriatic skin lesions caused by IMQ-induced PSO-like skin inflammation.

In this study, transcriptome sequencing of IMQ-induced psoriatic skin lesion tissues in mice was first performed to analyze the potential pathogenic mechanisms. The cream containing 5% BAI or 5% ECH or 5% combination of them (BAI/ECH = 1:1, 2:1, 1:2) was then prepared to explore the effects of BAI combined with ECH on psoriatic skin lesions. Network pharmacology and molecular docking were further performed to predict the potential targets and pathways of BAI and ECH by treating PSO on the skin. By combining transcriptome analysis with network pharmacology analysis, we measured the expressions of key cytokines and genes in skin lesion tissues related to potential targets and pathways in this study. A transgenic zebrafish model was then used to prove the effects of BAI combined with ECH and reveal the potential mechanism specifically.

2. MATERIALS AND METHODS

2.1. Chemicals and Reagents. Baicalin (BAI, HPLC 98%) and echinacoside (ECH, HPLC 98%) were purchased from Baoji Herbest Bio-Tech Co., Ltd. (Baoji, China). Vaseline, ethyl 4-hydroxybenzoate, triethanolamine, azone, glyceryl monostearate, copper sulfate pentahydrate ($CuSO_4 \cdot 5H_2O$), and tricaine were bought from Shanghai Aladdin Biochemical Technology Co., Ltd. (Shanghai, China). Glycerol and octadecanoic acid were obtained from Sinopharm Chemical Reagent Co., Ltd. (Shanghai, China). Halometasone (HMS) cream was provided by Bright Future Pharmaceuticals (Hong Kong, China). Imiquimod (IMQ) cream was supplied by iNova Pharmaceuticals (Singapore). Anti-PCNA Mouse mAb, anti-CD4 Rabbit pAb, and anti-CD68 Rabbit pAb were purchased from Servicebio Technology (Wuhan, China). The BCA protein assay kit was obtained from Beyotime (Shanghai, China). Mouse ELISA kits of tumor necrosis factor-α (TNF-α), interleukin-17A (IL-17A), interleukin-23 (IL-23), interleukin-10 (IL-10), and vascular endothelial growth factor A (VEGF-A), matrix metalloproteinase 9 (MMP-9), thioredoxin reductase (TrxR), and malondialdehyde (MDA) were bought from Nanjing SenBeiJia Biological Technology Co., Ltd. (Nanjing, China). Dexamethasone (DEX) and pronase E were supplied by Shanghai Yuanye Bio-Technology Co., Ltd. (Shanghai, China). The VEGF receptor tyrosine kinase inhibitor (VRI) was purchased from MCE (New Jersey).

2.2. Transcriptome Sequencing of Imiquimod (IMQ)-Induced Psoriatic Skin Lesion Tissues in Mice. An IMQ-induced psoriatic skin lesion in BALB/c mice is a classic disease model to study PSO.[21] To investigate the potential mechanism of IMQ-induced skin lesions in mice, transcriptome sequencing of the skin lesion tissues was then performed. Total RNA was isolated from skin lesion tissues in the normal control group (Con) and IMQ group separately. Each group contained three biological replications. Library construction and transcriptome sequencing were performed by BGI-Wuhan (Wuhan, China). Differentially expressed genes (DEGs) were screened out, and then, KEGG pathway enrichment analysis and GSEA analysis for DEGs between Con and IMQ groups were further analyzed.

2.3. Cream Preparation for the Experiment. In the cream preparation, the best preparation processes were optimized by a multifactor orthogonal test (Supporting Information 1). The content of triethanolamine (factor A) and glyceryl monostearate (factor B), emulsification temperature (factor C), and emulsification time (factor D) were taken as investigation factors to optimize the preparation of cream according to the evaluation criteria such as appearance quality, pH, centrifugal stability, heat-resistant stability, and cold-resistant stability (Tables S1−S4). The optimized cream was then prepared in this study.

The cream formulation includes the oil phase and aqueous phase. The oil phase consists of the following ingredients: octadecanoic acid (9.5%), glyceryl monostearate (5%), and vaseline (4%). The aqueous phase contains the following ingredients: triethanolamine (5%), glycerol (5.5%), azone (2%), BAI or ECH or a combination of them with different ratios (5%), ethyl 4-hydroxybenzoate (0.09%), and purified water. BAI and ECH can completely dissolve in the aqueous phase under the heating condition. Finally, the cream preparation is completed with purified water.

The preparation of cream is performed by adding the oil phase into the aqueous phase to form an emulsion. Specifically, the ingredients of the oil phase are first mixed at 80 °C until complete melting. The blend is then added into the aqueous phase, which is also heated at 80 °C. First, the mixture is continually stirred for 15 min. After the mixture is cooled to 40 °C, it is again continually stirred for 15 min to form the emulsion. After the emulsion is cooled to room temperature, a cream containing 5% BAI or 5% ECH or 5% combination of them (BAI/ECH = 1:1, 2:1, 1:2) is finished. The vehicle cream is prepared in the same way without adding BAI or ECH or a combination of them into the aqueous phase.

2.4. Animal Experiment and Drug Treatment. In this study, 8-week-old female BALB/c mice (16−19 g) were bought from Zhejiang Vital River Laboratory Animal Technology Co., Ltd. (Jiaxing, China, Certification No. 20220602Abzz0619000465). They were raised in a standardized laboratory animal center with free access to forage and water. The experimental manipulations were performed according to the National Institutes of Health Guidelines on Laboratory Research and approved by the Animal Ethics Committee of Hospital of Dermatology, Chinese Academy of Medical Sciences & Peking Union Medical College (Permit Number: 2022-DW-011).

72 mice were divided into 9 experimental groups (n = 8/each group): normal control group (Con), IMQ-induced

https://doi.org/10.1021/acsomega.3c04281
ACS Omega 2023, 8, 40260−40276

model group (IMQ), vehicle control group (KB), halometasone treatment group (HMS), 5% BAI cream treatment group (BAI), 5% ECH cream treatment group (ECH), 5% combination-1 (BAI/ECH = 1:1) cream treatment group (B1-E1), 5% combination-2 (BAI/ECH = 2:1) cream treatment group (B2-E1), and 5% combination-3 (BAI/ECH = 1:2) cream treatment group (B1-E2). 5% IMQ cream with a dose of 62.5 mg/d was topically applied on the shaved back (2 × 3 cm) of each mouse to induce psoriatic skin lesions in other groups except for the Con group. After topically administered with IMQ cream for 4 h, other groups were then applied with a dosage of cream the same as IMQ. All treatments required 6 consecutive days. The severity of skin lesions was evaluated using the Psoriasis Area and Severity Index (PASI) score system. These skin lesion tissues were then collected for further study.

2.5. Histological and Immunohistochemical Analysis. The skin lesion tissues in each group were fixed in 4% paraformaldehyde and embedded in paraffin wax. The paraffin sections (5 μm) were stained with hematoxylin−eosin (HE) and then observed by an upright fluorescence microscope (OLYMPUS, Japan). Image-Pro Plus 6.0 software was further used to measure the epidermal thickness. Meanwhile, the proliferation of epidermal keratinocytes in skin lesion tissues was detected by immunohistochemistry (IHC) staining with anti-PCNA Mouse mAb. In addition, the $CD4^+$ T cell infiltration and macrophage infiltration in these skin lesion tissues were also detected by IHC staining of anti-CD4 Rabbit pAb and anti-CD68 Rabbit pAb, respectively. Furthermore, the IHC staining intensity was then measured by Image-Pro Plus 6.0 software.

2.6. Potential Targets and Pathways of BAI and ECH Treating Psoriasis Focused on the Skin by Network Pharmacology Analysis. *2.6.1. Target Collection.* GeneCards, DisGeNET, and MalaCards databases were used to collect disease targets of PSO. PharmMapper, SEA, and SIB databases were used to obtain the potential targets of BAI and ECH. Venn diagram analysis was performed to screen out the potential targets of BAI treating PSO and ECH treating PSO. The TiGER database, a database for tissue-specific gene expression and regulation, was then used to verify the skin tissue-specific gene expression and regulation of these targets.[22]

2.6.2. Construction of a Compound−Target Network. The STRING database was first used to obtain the interaction relationship of these targets with skin tissue-specific gene expression and regulation. The compound−target network was then constructed by Cytoscape 3.7.2 software. In the graphical network, the degree value of a node indicates the number of connections between the node and the other nodes. Furthermore, the key targets were validated by molecular docking. Molecular docking between key target proteins and BAI or ECH was performed with AutoDock Vina. PyMOL software was then used to visualize the results of molecular docking.

2.6.3. Enrichment Analysis. Enrichment analysis of the GO biological process was performed by FunRich software, and the significant functional annotation was determined with a corrected *P*-value of less than 0.05. KEGG pathway enrichment analysis was conducted by the KOBAS database, and the significant functional annotation was also confirmed with a corrected *P*-value of less than 0.05.

2.7. Biochemical Test of Skin Lesion Tissues in Mice by ELISA. After removing fat parts, the skin lesion tissues were weighed and cut into pieces. These tissues were homogenized according to the ratio of 1:9 (tissue weight/PBS volume) and then centrifuged at 4 °C at 4000 rpm for 10 min. The supernatant was collected and diluted to measure the protein concentration by the BCA method. According to the instructions of ELISA kits; the levels of TNF-α, IL-17A, IL-23, and IL-10 and the contents of VEGF-A, MMP-9, and MDA; and the activity of TrxR in skin lesion tissues were measured by a microplate reader (TECAN, Switzerland).

2.8. Zebrafish Experiments and Drug Treatment. *2.8.1. Maintenance of Zebrafish Embryos.* Neutrophil-specific transgenic (mpx:EGFP) zebrafish embryos labeled with the enhanced green fluorescent protein in neutrophils and vessel-specific transgenic (fli1:EGFP) zebrafish embryos labeled with green fluorescence in vessels were bought from EzeRinka (Nanjing, China). These embryos were maintained in zebrafish embryo water and raised at 28.5 °C on a 14 h light/10 h dark cycle in a healthy state for further experiments.

2.8.2. Evaluation of the Anti-Inflammatory Effect of BAI and ECH on $CuSO_4$-Induced Inflammation Model in Tg (mpx:EGFP) Transgenic Zebrafish. $CuSO_4$, DEX, BAI, ECH, B1-E1 (BAI/ECH = 1:1), B2-E1 (BAI/ECH = 2:1), and B1-E2 (BAI/ECH = 1:2) were separately solubilized in a suitable volume of DMSO and diluted to the required concentration with embryo water for the assay.

Tg (mpx:EGFP) zebrafish larvae at 3 days post fertilization (dpf) were randomly assigned into a 24-well plate with 10 larvae per well. A $CuSO_4$-induced inflammation model in Tg (mpx:EGFP) zebrafish larvae was performed as described in previous studies.[23−25] 18 experimental groups (10 larvae/each group) were shown as follows: 0.1% DMSO (normal control group, Ctrl), 3.2 μg/mL $CuSO_4$ (model group, $CuSO_4$), 5 μg/mL DEX (positive control group, DEX), 25, 50, and 100 μg/mL BAI (BAI treatment groups, BAI_25, BAI_50, and BAI_100, respectively), 25, 50, and 100 μg/mL ECH (ECH treatment groups, ECH_25, ECH_50, and ECH_100, respectively), 25, 50, and 100 μg/mL B1-E1 (B1-E1 treatment groups, B1-E1_25, B1-E1_50, and B1-E1_100, respectively), 25, 50, and 100 μg/mL B2-E1 (B2-E1 treatment groups, B2-E1_25, B2-E1_50, and B2-E1_100, respectively), and 25, 50, and 100 μg/mL B1-E2 (B1-E2 treatment groups, B1-E2_25, B1-E2_50, and B1-E2_100, respectively). Except for the Ctrl group, Tg (mpx:EGFP) zebrafish larvae in other groups were first treated with 3.2 μg/mL $CuSO_4$ for 2 h. Next, $CuSO_4$ was washed out, and drug treatment groups were then treated with corresponding drugs for 6 h, and the model group was treated with 0.1% DMSO. Notably, the solution volume per well was 2 mL. After the treatments, Tg (mpx:EGFP) zebrafish larvae in each group were washed with embryo water and anesthetized with 0.02% tricaine. The fluorescence in Tg (mpx:EGFP) zebrafish larvae was then observed and photographed by an upright fluorescence microscope (OLYMPUS, Japan). Meanwhile, Image-Pro Plus 6.0 software was used to quantify the recruitment of neutrophils to the inflammatory site in zebrafish larvae. The ratio of inflammatory inhibition was then calculated based on the number of neutrophils recruited (N), and the calculation formula is as follows: inflammatory inhibition (%) = { [N (model group) − N (drug treatment group)]/[N (model group) − N (normal control group)] } × 100%.

To measure the expression of inflammation-related genes in the $CuSO_4$-induced inflammation model and drug treatment groups, quantitative real-time PCR (qPCR) was further

https://doi.org/10.1021/acsomega.3c04281
ACS Omega 2023, 8, 40260−40276

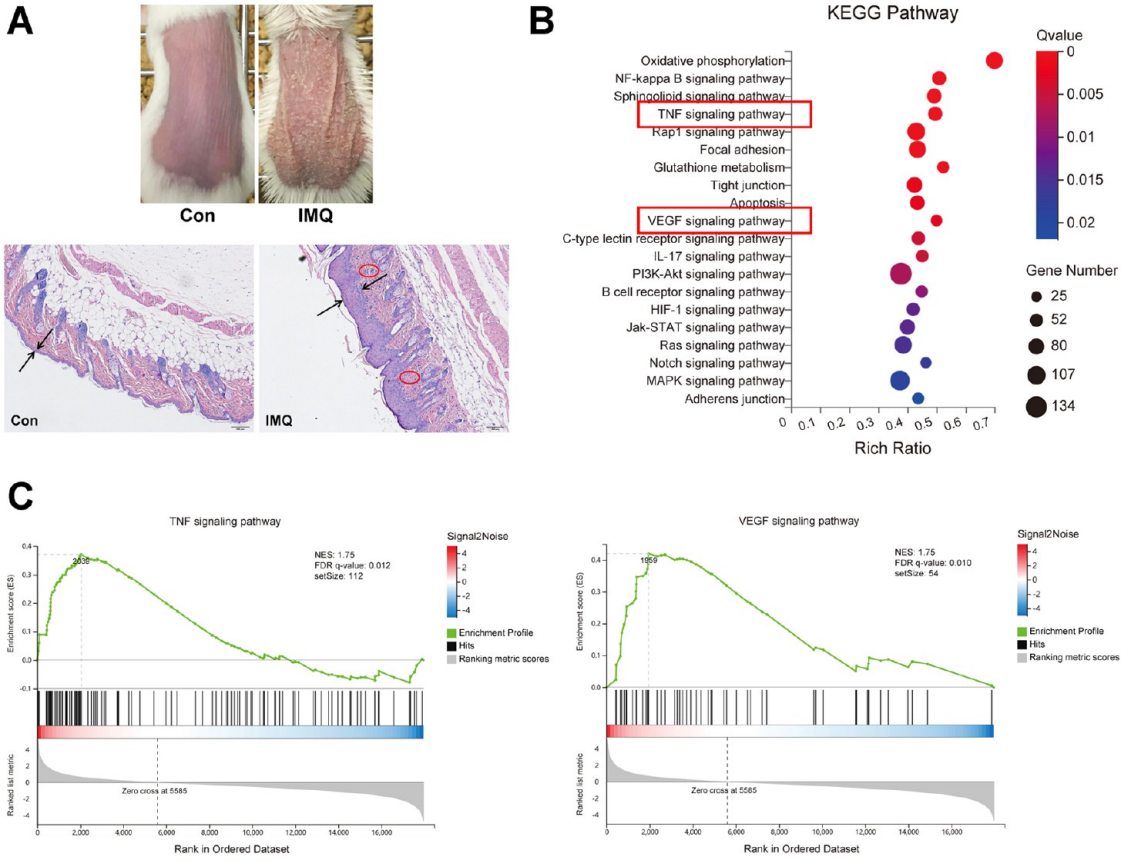

Figure 1. Transcriptome analysis of skin lesion tissues from Con and IMQ groups. (A) Representative pictures of dorsal skin and histopathological observation of skin lesions by HE staining (scale bar, 100 μm) between Con and IMQ groups after topical application of IMQ for 6 days. Two opposite arrows indicated the epidermis, and the red circle indicated the inflammatory cell infiltration. (B) KEGG pathway enrichment analysis of DEGs between Con and IMQ groups. (C) Gene set enrichment analysis (GSEA) of the TNF signaling pathway and the VEGF signaling pathway.

performed. Tg (mpx:EGFP) zebrafish larvae at 3 dpf were randomly distributed into a 24-well plate with 10 larvae per well. Seven experimental groups (20 larvae/each group) were set as follows: 0.1% DMSO (Ctrl), 3.2 μg/mL $CuSO_4$ ($CuSO_4$), 100 μg/mL BAI (BAI_100), 100 μg/mL ECH (ECH_100), 100 μg/mL B1-E1 (B1-E1_100), 100 μg/mL B2-E1 (B2-E1_100), and 100 μg/mL B1-E2 (B1-E2_100). After the induction of $CuSO_4$ and drug treatment described above, Tg (mpx:EGFP) zebrafish larvae in each group were washed with embryo water and then collected for the qPCR assay.

2.8.3. Evaluation of the Antiangiogenic Effect of BAI and ECH in Tg (fli1:EGFP) Transgenic Zebrafish. VRI, BAI, ECH, B1-E1 (BAI/ECH = 1:1), B2-E1 (BAI/ECH = 2:1), and B1-E2 (BAI/ECH = 1:2) were separately solubilized in a suitable volume of DMSO and diluted to the required concentration with embryo water for the assay.

First, Tg (fli1:EGFP) zebrafish embryos at 24 h post fertilization (hpf) were treated with 1 mg/mL pronase E to remove the embryo membrane. Next, these zebrafish larvae were randomly transferred into a 24-well plate with 10 larvae per well. The antiangiogenic experiment in Tg (fli1:EGFP) zebrafish larvae was performed as the previous studies.[26,27] 17 experimental groups (10 larvae/each group) were shown as follows: 0.1% DMSO (normal control group, Ctrl), 600 ng/mL VRI (positive control group, VRI), 25, 50, and 100 μg/mL BAI (BAI treatment groups, BAI_25, BAI_50, and BAI_100, respectively), 25, 50, and 100 μg/mL ECH (ECH treatment groups, ECH_25, ECH_50, and ECH_100, respectively), 25, 50, and 100 μg/mL B1-E1 (B1-E1 treatment groups, B1-E1_25, B1-E1_50, and B1-E1_100, respectively), 25, 50, and 100 μg/mL B2-E1 (B2-E1 treatment groups, B2-E1_25, B2-E1_50, and B2-E1_100, respectively), and 25, 50, snd 100 μg/mL B1-E2 (B1-E2 treatment groups, B1-E2_25, B1-E2_50, and B1-E2_100, respectively). Except for the Ctrl group, Tg (fli1:EGFP) zebrafish larvae in other groups were treated with corresponding drugs for 24 h. The solution volume per well was 2 mL. After the treatments, Tg (fli1:EGFP) zebrafish larvae in each group were washed with embryo water and anesthetized with 0.02% tricaine. The zebrafish larvae were placed laterally on glass slides, and the intersegmental blood vessels (ISVs) were then imaged by using an upright fluorescence microscope (OLYMPUS, Japan). Intact vessels were defined as ISVs that connected the dorsal aorta (DA) to the posterior cardinal vein (PCV) and elongated to the dorsal longitudinal anastomotic vessels (DLAVs).[28] The antiangiogenic activity was evaluated by both the intact and defective ISVs. Image-Pro Plus 6.0 software was then used to count the number of intact and defective ISVs. The ISVs index is calculated as follows: ISVs index = number of intact vessels × 1 + number of defective vessels × 0.5.[29] The ratio of angiogenic inhibition was then calculated based on the ISVs index, and the calculation formula is as follows: angiogenic inhibition (%) = { [ISVs index (Ctrl group) − ISVs index (drug treatment group)]/ISVs index (Ctrl group) } × 100%.

qPCR was also performed to analyze the expression of angiogenesis-related genes in the drug treatment groups. Tg

https://doi.org/10.1021/acsomega.3c04281
ACS Omega 2023, 8, 40260−40276

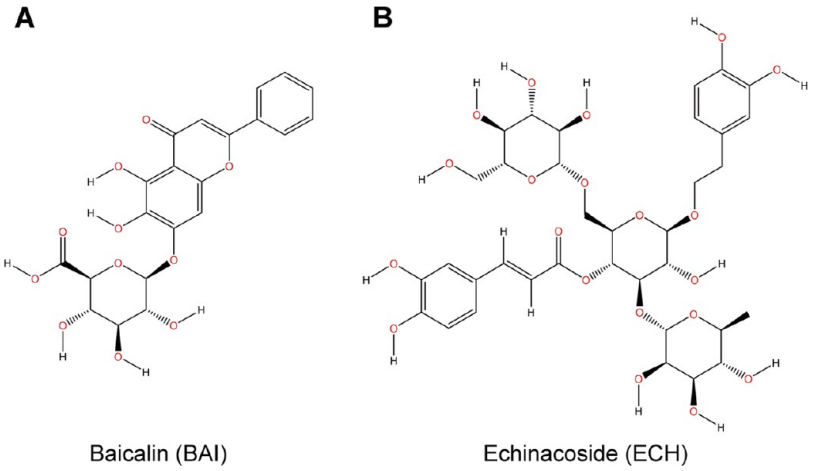

Figure 2. Chemical structures of (A) baicalin (BAI) and (B) echinacoside (ECH).

(fli1:EGFP) zebrafish embryos at 24 hpf were treated with 1 mg/mL pronase E and then transferred into a 24-well plate with 10 larvae per well. Seven experimental groups (20 larvae/each group) were set as follows: 0.1% DMSO (Ctrl), 600 ng/mL VRI (VRI), 100 μg/mL BAI (BAI_100), 100 μg/mL ECH (ECH_100), 100 μg/mL B1-E1 (B1-E1_100), 100 μg/mL B2-E1 (B2-E1_100), and 100 μg/mL B1-E2 (B1-E2_100). As the experimental method mentioned above, Tg (fli1:EGFP) zebrafish larvae in each group were washed with embryo water and then collected for the qPCR assay.

2.9. Quantitative Real-Time PCR. Total RNA from skin lesion tissues and zebrafish larvae was extracted using TRIzol (Accurate Biology, China) and then transcribed into cDNAs. qPCR was performed by a Roche Light Cycler 480 QPCR System (Roche, Switzerland) with a thermal profile of 95 °C for 30 s and 40 cycles of 95 °C for 5 s and 60 °C for 30 s. The primer sequences for mRNA expression measured in mice are listed in Table S5, and the primer sequences for detecting mRNA expression in zebrafish larvae are listed in Table S6. All of the primers were synthesized by Sangon Biotech (Shanghai) Co., Ltd. (Shanghai, China). The data were standardized to the expression level of β-actin. Relative mRNA expression levels were calculated using the $2^{-\triangle\triangle CT}$ method.

2.10. Statistical Analysis. Data are expressed as the mean ± SD. Data from multiple groups were assessed by one-way ANOVA followed by Sidak's multiple comparison test using GraphPad Prism. Student's *t*-test was used to analyze the data between two groups. $P < 0.05$ was considered statistically significant.

3. RESULTS AND DISCUSSION

3.1. Potential Pathogenic Mechanisms of IMQ-Induced Psoriatic Skin Lesions in Mice. As shown in Figure 1A, the phenotype of IMQ-induced psoriatic skin lesions in mice was significant compared to the Con group, particularly the epidermal thickness and inflammatory cell infiltration. Potential pathogenic mechanisms of IMQ-induced skin lesions were then investigated by transcriptome analysis of skin lesion tissues from Con and IMQ groups. As shown in Figure 1B, KEGG pathway enrichment analysis of DEGs between Con and IMQ groups indicated that the TNF signaling pathway and the VEGF signaling pathway were significantly enriched in IMQ-induced psoriatic skin lesions. The enrichment profiles of the TNF signaling pathway and the VEGF signaling pathway were then performed by Gene set enrichment analysis (GSEA). The results further showed the significance of the TNF signaling pathway and the VEGF signaling pathway in IMQ-induced skin lesions (Figure 1C).

The TNF signaling pathway, especially TNF-α, plays an important role in the development of psoriatic skin lesions.[30] TNF-α is a proinflammatory cytokine associated with the pathogenesis of PSO, and anti-TNF-α therapies are effective in PSO.[31] In recent years, it has been found that the increased level of proangiogenic factors and abnormal angiogenesis are closely associated with the development of PSO.[32] Angiogenesis and abnormal microvessels are important links in the pathogenesis of PSO, particularly vascular changes that precede epidermal hyperplasia in PSO.[33] Angiogenesis is closely related to the VEGF signaling pathway, especially the key target VEGFA.[34] It has been reported that VEGFA could promote the aggravation of PSO, and targeting VEGFA signaling in the epidermis could prevent the continued development of PSO.[35]

3.2. Topical Application of B2-E1 Had the Better Effects of Ameliorating IMQ-Induced Skin Lesions than the Single Component in Mice. BAI (Figure 2A) is the main active component of *S. baicalensis* with significant anti-inflammatory and antibacterial effects.[36] ECH (Figure 2B), an active component of *E. purpurea*, has significant antiangiogenesis and antioxidant effects.[16] Previous studies have shown that inflammation, angiogenesis, and oxidative stress were the key links in the pathogenesis of PSO.[37−39] Due to the anti-inflammatory effect of BAI, the antiangiogenic activity, and the antioxidant effect of ECH, it was proposed that the combination of BAI and ECH could better ameliorate the psoriatic skin lesions by their multiple pharmacological effects. Therefore, this study aimed to explore the potential effects and mechanisms of BAI combined with ECH on PSO by a topical treatment.

A cream containing 5% BAI or 5% ECH or 5% combination of them (BAI/ECH = 1:1, 2:1, 1:2) was prepared as the described methods mentioned above. As shown in Figure 3A,B, IMQ-induced skin lesions were significantly observed in the IMQ and KB groups. Topical application of HMS, BAI, ECH, B1-E1, B2-E1, and B1-E2 could notably alleviate the phenotype of skin lesions including erythema, scales, and thickness induced by IMQ and significantly decrease the cumulative score as compared to IMQ and KB groups ($P <$

https://doi.org/10.1021/acsomega.3c04281
ACS Omega 2023, 8, 40260−40276

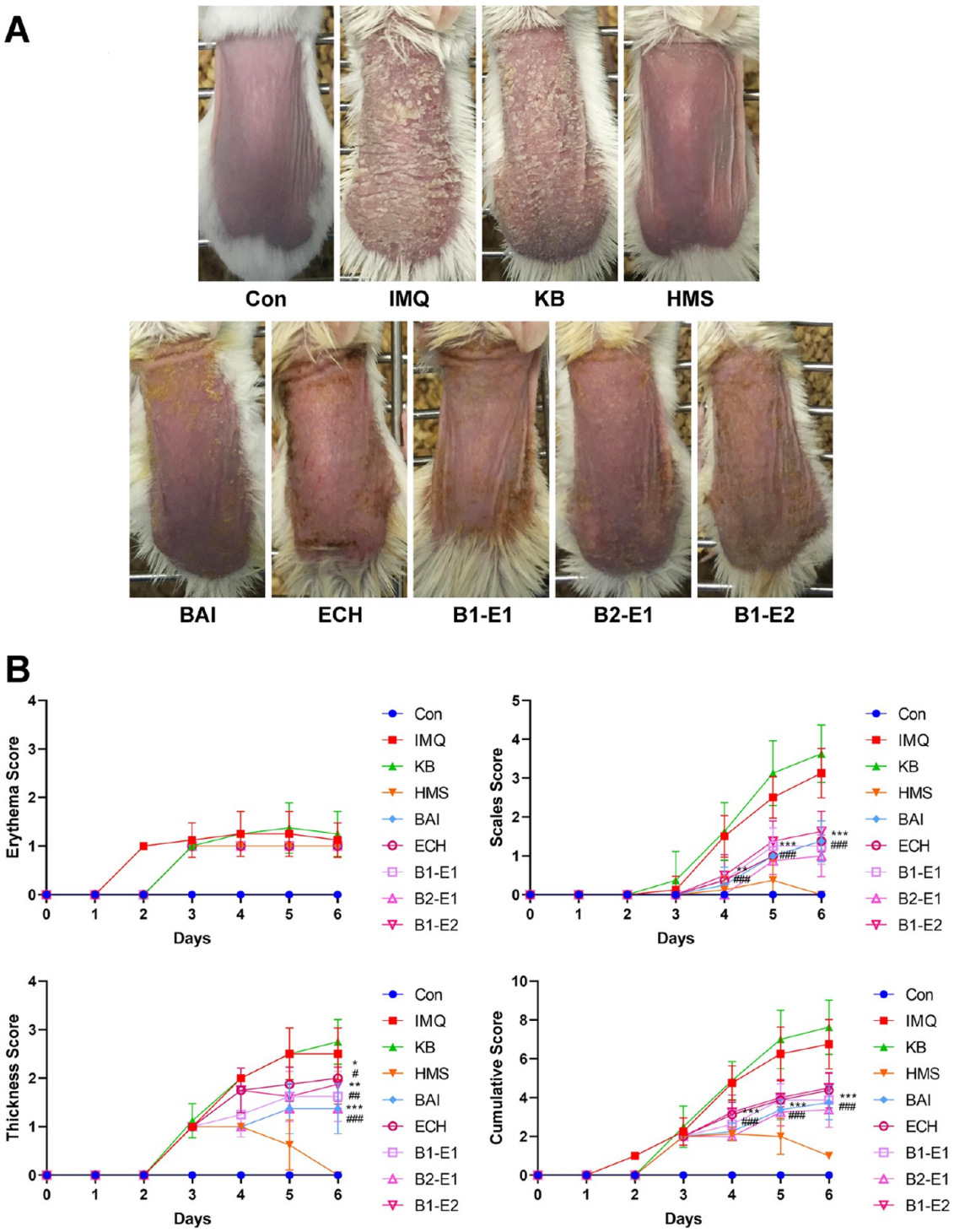

Figure 3. Topical application of BAI and ECH and a mixture of them (BAI/ECH = 1:1, 2:1, 1:2) alleviated the severity of psoriatic skin lesions induced by IMQ. (A) Representative photographs of dorsal skin in each group after the treatment for 6 days (n = 8). (B) Evaluation of the severity of skin lesions by PASI score, including erythema score, scales score, thickness score, and cumulative score (n = 8). Data are represented as mean ± SD. $^{\#}P < 0.05$, $^{\#\#}P < 0.01$, and $^{\#\#\#}P < 0.001$ versus the IMQ group and $^{*}P < 0.05$, $^{**}P < 0.01$, and $^{***}P < 0.001$ versus the KB group.

0.05, $P < 0.01$, $P < 0.001$). Meanwhile, histological observation and morphometric analysis of skin lesion tissues showed that HMS, BAI, ECH, B1-E1, B2-E1, and B1-E2 (drug treatment groups) could ameliorate the inflammatory cell infiltration and decrease the epidermal thickness as compared to IMQ and KB groups ($P < 0.001$), particularly the better effects of B2-E1 than those of the single component, B1-E1, and B1-E2 (Figure 4A,B).

In addition, IHC staining of PCNA, CD4, and CD68 in skin lesion tissues was also performed in this study. As shown in Figure 5A,B, drug treatment groups decreased the PCNA staining intensity of skin lesion tissues to a certain degree compared to that in IMQ and KB groups ($P < 0.05$, $P < 0.01$, $P < 0.001$), which indicated that drug treatment groups could inhibit the proliferation of epidermal keratinocytes. Furthermore, the inhibitory effect of B2-E1 was better than those of

https://doi.org/10.1021/acsomega.3c04281
ACS Omega 2023, 8, 40260−40276

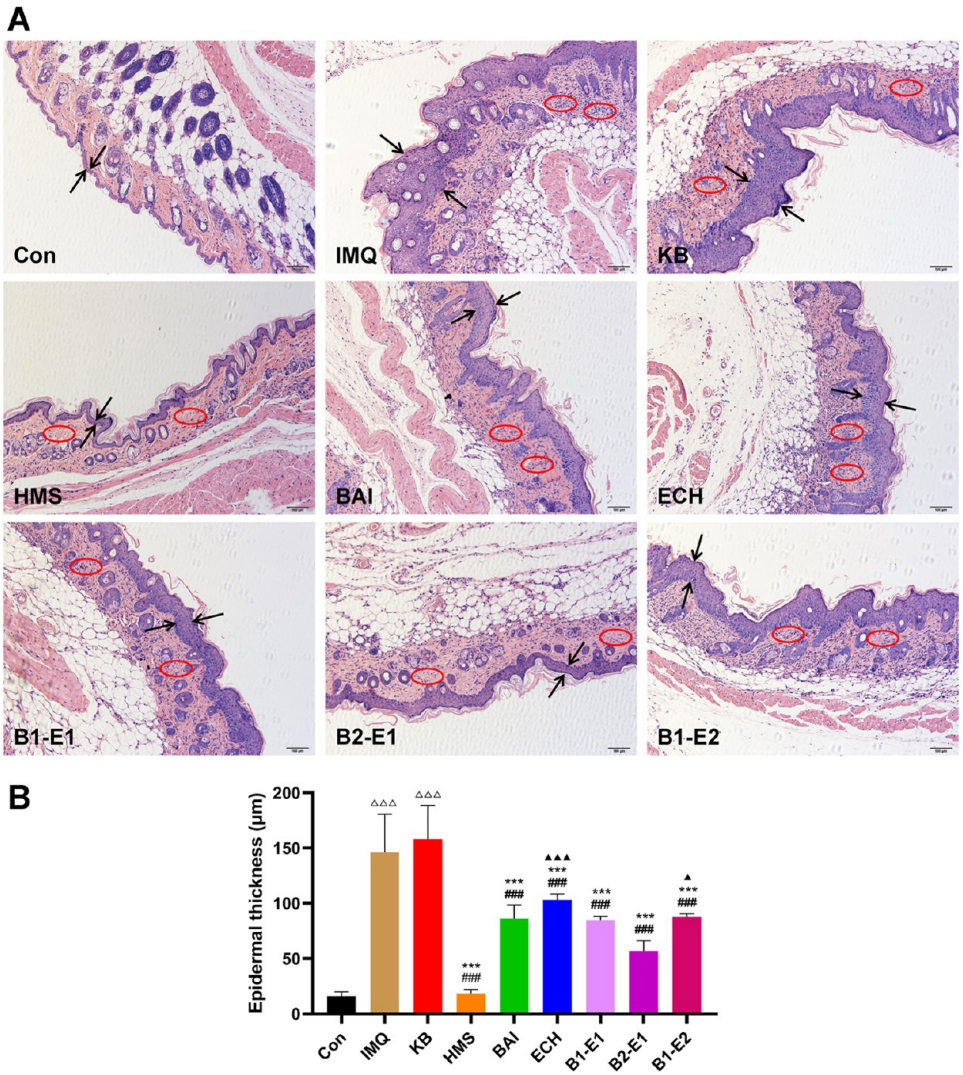

Figure 4. Topical application of BAI and ECH and a mixture of them (BAI/ECH = 1:1, 2:1, 1:2) decreased epidermal thickness and alleviated inflammatory cell infiltration in IMQ-induced psoriatic skin lesions. (A) Representative images of HE-stained skin lesion tissues in each group (scale bar, 100 μm, n = 8). Two opposite arrows indicated the epidermis, and the red circle indicated the inflammatory cell infiltration. (B) Statistical analysis of the epidermal thickness of skin lesion tissues in each group measured by Image-Pro Plus 6.0 software (n = 8). Data are expressed as mean ± SD $^{\triangle\triangle\triangle}P < 0.001$ versus the Con group, $^{\#\#\#}P < 0.001$ versus the IMQ group, $^{***}P < 0.001$ versus the KB group, and $^{\blacktriangle}P < 0.05$ and $^{\blacktriangle\blacktriangle\blacktriangle}P < 0.001$ versus the B2-E1 group.

the single component, B1-E1, and B1-E2, particularly significant compared to the ECH and B1-E2 groups ($P < 0.05$, $P < 0.001$). As shown in Figure 6A–C, drug treatment groups obviously decreased the CD4 staining intensity and CD68 staining intensity of skin lesion tissues compared to the IMQ and KB groups ($P < 0.001$), which indicated that drug treatment groups could alleviate $CD4^+$ T cell infiltration and macrophage infiltration in skin lesion tissues. In the statistical analysis of CD4 staining intensity, the effect of B2-E1 was better than those of the single component, B1-E1, and B1-E2, particularly significant compared to BAI, ECH, and B1-E2 groups ($P < 0.05$, $P < 0.01$, $P < 0.001$). In the statistical analysis of CD68 staining intensity, the effect of B2-E1 was also better than those of the single component, B1-E1, and B1-E2, particularly significant compared to the ECH group ($P < 0.05$).

3.3. B2-E1 Suppressed the TNF Signaling Pathway and the VEGF Signaling Pathway Better than the Single Component in IMQ-Induced Mice. According to the experimental results shown above, topical application of BAI combined with ECH could significantly ameliorate IMQ-induced psoriatic skin lesions in mice, particularly the effects of B2-E1 (BAI/ECH = 2:1). To further explore the potential mechanisms of topical BAI treating PSO and topical ECH treating PSO, network pharmacology and molecular docking were then performed in this study (Supporting Information 3). The prediction results showed that BAI may treat PSO on the skin by regulating the TNF signaling pathway, especially acting on TNF and AKT1. Meanwhile, ECH may treat PSO on the skin by regulating the VEGF signaling pathway, particularly acting on VEGFA and MMP9. By combining with the transcriptome analysis, it suggested that BAI combined with ECH may regulate the TNF signaling pathway and the VEGF signaling pathway on the topical treatment of PSO.

It has been reported that TNF-α is the key target of the TNF signaling pathway, which can mediate the inflammatory response, particularly the release of inflammatory cytokines.[40] Previous studies have suggested that the IL-23/IL-17A/IL-22 cytokine axis played an important role in the pathogenesis of

https://doi.org/10.1021/acsomega.3c04281
ACS Omega 2023, 8, 40260−40276

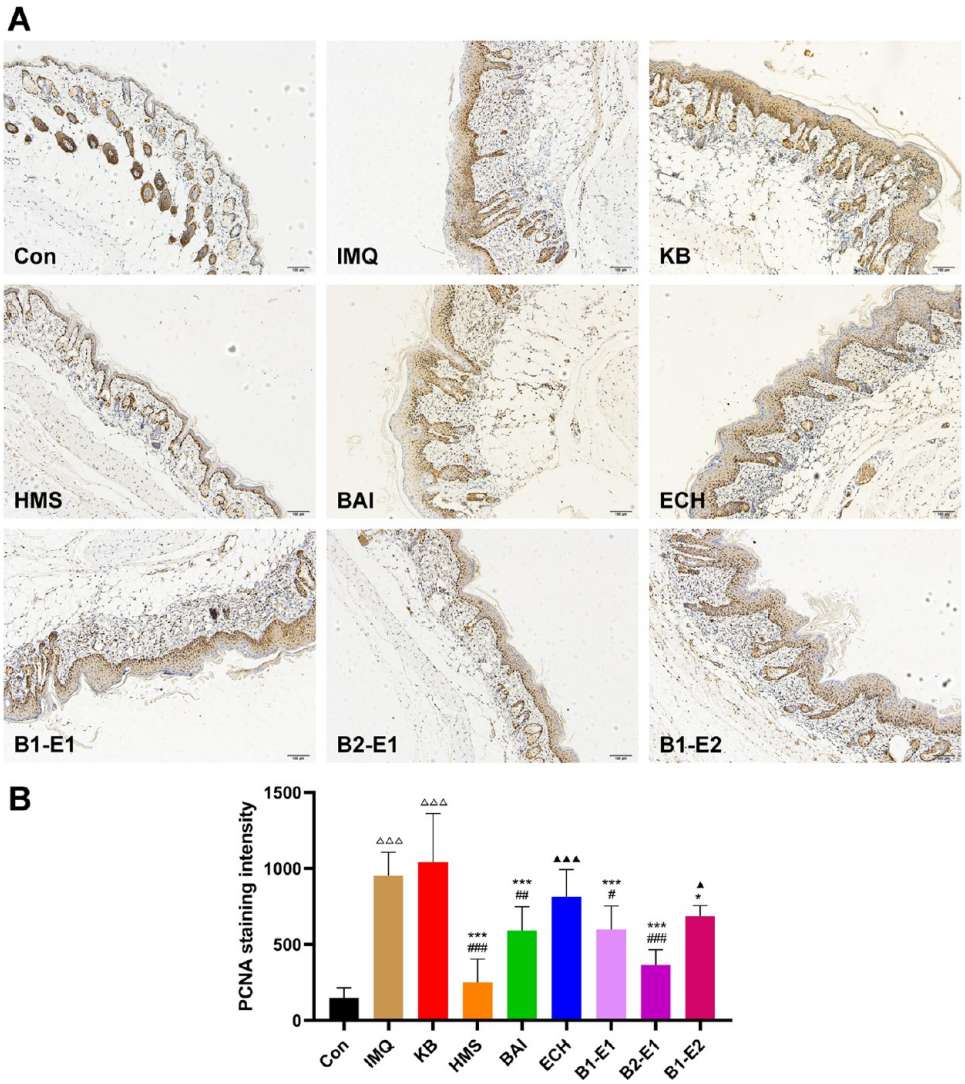

Figure 5. Topical application of BAI and ECH and a mixture of them (BAI/ECH = 1:1, 2:1, 1:2) inhibited the proliferation of epidermal keratinocytes in skin lesion tissues. (A) Representative photographs of IHC staining of anti-PCNA Mouse mAb in skin lesion tissues in each group (scale bar, 100 μm, n = 6). (B) Statistical analysis of the PCNA staining intensity of epidermal keratinocytes in skin lesion tissues in each group measured by Image-Pro Plus 6.0 software (n = 6). Data are represented as mean ± SD $^{\triangle\triangle\triangle}P < 0.001$ versus the Con group, $^{\#}P < 0.05$, $^{\#\#}P < 0.01$, and $^{\#\#\#}P < 0.001$ versus the IMQ group, $^{*}P < 0.05$ and $^{***}P < 0.001$ versus the KB group, and $^{\blacktriangle}P < 0.05$ and $^{\blacktriangle\blacktriangle\blacktriangle}P < 0.001$ versus the B2-E1 group.

psoriasis.[41] In the development of psoriatic skin lesions, myeloid dendritic cells are activated and secrete inflammatory cytokines such as IL-12 and IL-23.[42] IL-12 induces the differentiation of initial T cells into Th1 cells, while IL-23 plays an important role in the survival and proliferation of Th17 and Th22 cells.[43] Th1 cells secrete IFN-γ and TNF-α. Th17 cells secrete IL-17A, IL-22, and TNF-α. These cytokines can induce keratinocyte proliferation, increase the expression of angiogenic mediators and endothelial adhesion molecules, and cause immune cells to infiltrate into skin lesions.[44] In addition, IL-10 is an important anti-inflammatory cytokine that can regulate the response of the immune system in psoriasis.[45] As shown in Figure 7A, the levels of TNF-α, IL-17A, and IL-23 in skin lesion tissues were significantly increased (P<0.001), and the content of IL-10 was obviously decreased (P<0.001) in IMQ and KB groups as compared to the Con group. Compared with IMQ and KB groups, drug treatment groups could decrease the content of TNF-α, IL-17A, and IL-23 and increase the level of IL-10 to a certain degree ($P < 0.05$, $P < 0.01$, $P < 0.001$). Furthermore, the effect of B2-E1 was better than those of the single component, B1-E1, and B1-E2, particularly significant compared to the ECH group in the statistical analysis of IL-23 content ($P < 0.01$).

VEGFA (VEGF-A) is the key target of the VEGF signaling pathway, which is closely associated with angiogenesis.[46] In addition, angiogenesis is also closely related to MMP9 (MMP-9), which can participate in angiogenesis by releasing VEGF.[47] Furthermore, the regulation of angiogenesis is also closely related to the antioxidant effect.[48] Therefore, the angiogenesis-related cytokine VEGF-A and MMP-9 and antioxidant ability, such as TrxR activity and MDA content, were measured by the ELISA test. As shown in Figure 7B, the content of VEGF-A and MMP-9 in skin lesion tissues was significantly increased (P<0.001) in the IMQ and KB groups compared to the Con group. Compared with IMQ and KB groups, drug treatment groups could obviously decrease the levels of VEGF-A and MMP-9 ($P < 0.05$, $P < 0.01$, $P < 0.001$). Particularly, the effect of B2-E1 was significant compared to the BAI group ($P <$

https://doi.org/10.1021/acsomega.3c04281
ACS Omega 2023, 8, 40260−40276

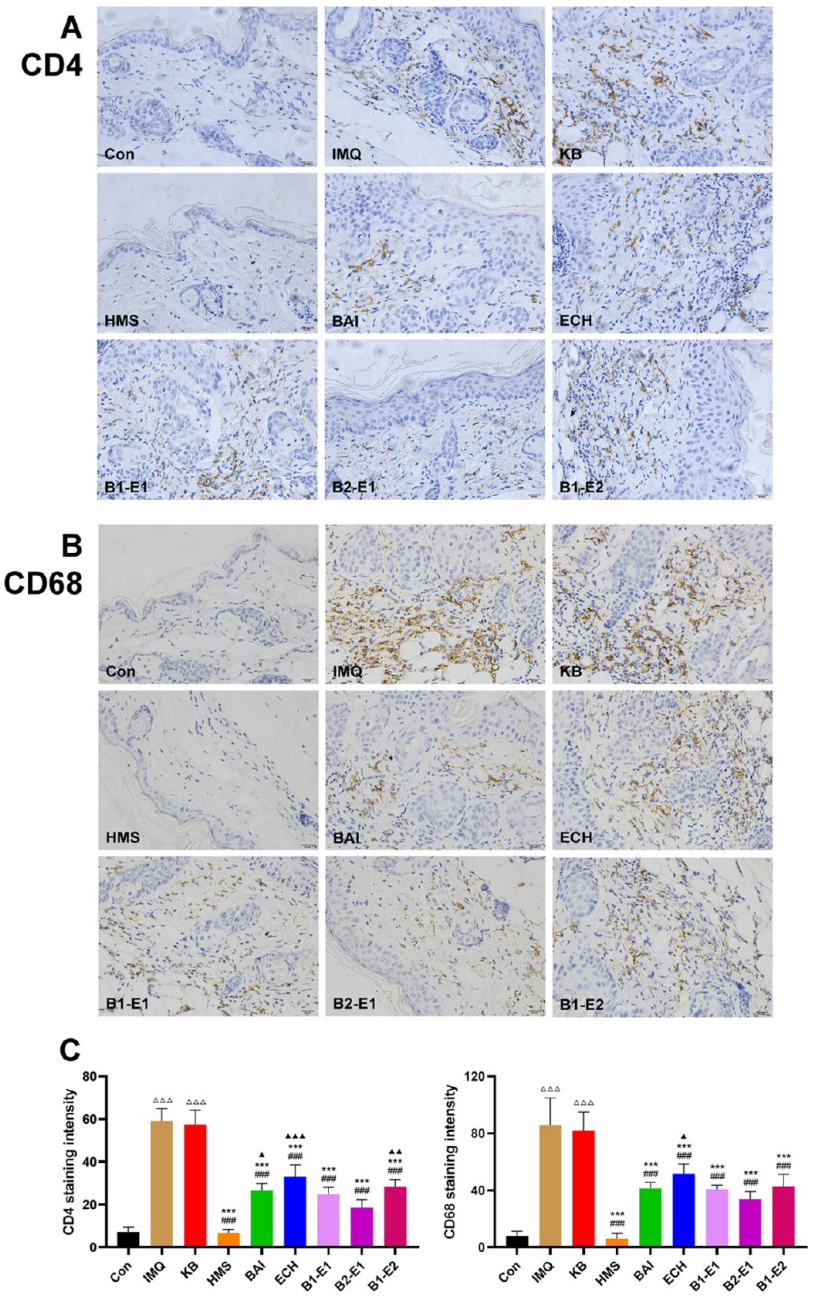

Figure 6. Topical application of BAI and ECH and a mixture of them (BAI/ECH = 1:1, 2:1, 1:2) ameliorated the $CD4^+$ T cells infiltration and macrophage infiltration in IMQ-induced psoriatic skin lesion tissues. (A) Representative pictures of IHC staining of anti-CD4 Rabbit pAb in skin lesion tissues in each group (scale bar, 20 μm, $n = 6$). (B) Representative pictures of IHC staining of anti-CD68 Rabbit pAb in skin lesion tissues in each group (scale bar, 20 μm, $n = 6$). (C) Statistical analysis of CD4 staining intensity and CD68 staining intensity in skin lesion tissues in each group measured by Image-Pro Plus 6.0 software ($n = 6$). Data are expressed as mean ± SD $^{\triangle\triangle\triangle}P < 0.001$ versus the Con group, $^{\#\#\#}P < 0.001$ versus the IMQ group, $^{***}P < 0.001$ versus the KB group, and $^{\blacktriangle}P < 0.05$, $^{\blacktriangle\blacktriangle}P < 0.01$, and $^{\blacktriangle\blacktriangle\blacktriangle}P < 0.001$ versus the B2-E1 group.

0.01). Meanwhile, TrxR activity was notably decreased, and MDA content was obviously increased in the IMQ and KB groups compared to the Con group. Compared with the IMQ and KB groups, drug treatment groups could significantly increase TrxR activity and decrease MDA content ($P < 0.01$, $P < 0.001$). Particularly, the effect of B2-E1 was also significant compared to the BAI group in the statistical analysis of MDA content ($P < 0.01$).

To further study the regulation of the TNF signaling pathway and the VEGF signaling pathway for topical application of BAI combined with ECH treating IMQ-induced psoriatic skin lesions, the relative mRNA expressions of 12 key genes involved in the TNF signaling pathway and the VEGF signaling pathway based on network pharmacology analysis were then measured by qPCR (Figure 8A,B). In these key target genes of the TNF signaling pathway, TNF (TNF-α) is an important proinflammatory mediator that can stimulate the inflammatory response.[49] AKT1 is also a potential specific target for relieving inflammation.[50] Furthermore, targeting CCL5 may decrease inflammatory responses in various allergic, autoimmune, or infectious diseases.[51] In addition, MMP3 plays an important role in the inflammatory signaling pathway, and CASP7 and MAPK14 also participate in the processes of inflammation.[52−54] In this study, BAI combined with ECH

https://doi.org/10.1021/acsomega.3c04281
ACS Omega 2023, 8, 40260−40276

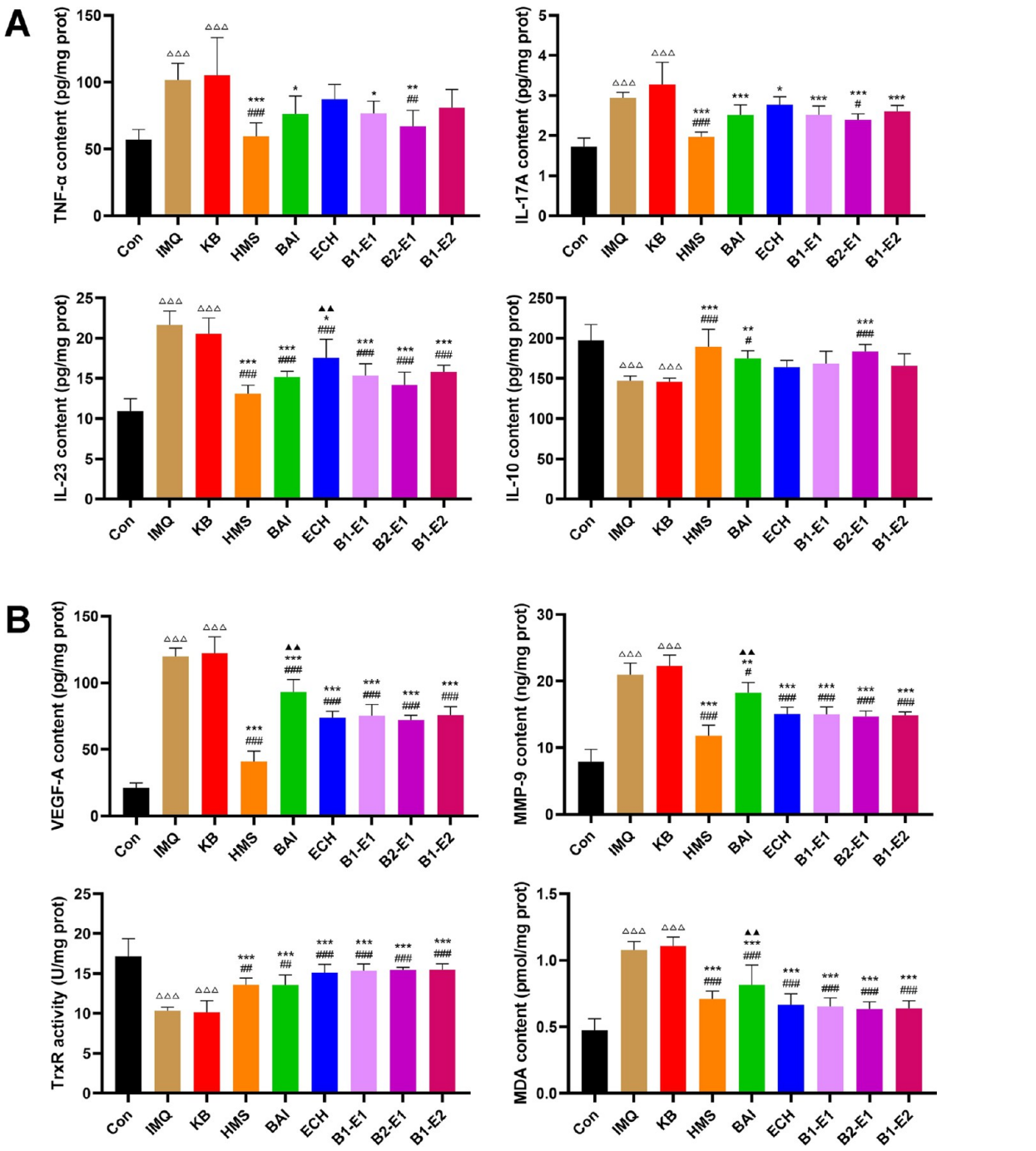

Figure 7. Topical application of B2-E1 (BAI/ECH = 2:1) reduced the release of inflammatory factors including TNF-α, IL-17A, and IL-23, increased the anti-inflammatory cytokine IL-10, inhibited the angiogenesis-related cytokine VEGF-A and MMP-9, and improved the antioxidant ability better than the single component in IMQ-induced psoriatic skin lesions. (A) The levels of TNF-α, IL-17A, IL-23, and IL-10 in skin lesion tissues in each group (n = 6). (B) The content of VEGF-A and MMP-9, the activity of TrxR, and the content of MDA in skin lesion tissues in each group (n = 6). Data are represented as mean ± SD $^{\triangle\triangle\triangle}P < 0.001$ versus the Con group, $^{\#}P < 0.05$, $^{\#\#}P < 0.01$, and $^{\#\#\#}P < 0.001$ versus the IMQ group, $^{*}P < 0.05$, $^{**}P < 0.01$, and $^{***}P < 0.001$ versus the KB group, and $^{\blacktriangle\blacktriangle}P < 0.01$ versus the B2-E1 group.

could potently reverse the mRNA expression of these key genes in the TNF signaling pathway, especially the better effect of B2-E1 than those of the single component, B1-E1, and B1-E2. In these key target genes of the VEGF signaling pathway, VEGFA and MMP9 are all closely associated with angiogenesis.[46,47] SRC also plays an important role in the control of angiogenesis.[55] In addition, the angiogenesis-related genes also include NOS3, MAP2K1, and CDC42.[56−58] In the present study, BAI combined with ECH could significantly reverse the mRNA expression of these key genes in the VEGF signaling pathway, especially the better effect of B2-E1 than those of the single component, B1-E1, and B1-E2.

3.4. B2-E1 Inhibited $CuSO_4$-Induced Neutrophil Migration Better than the Single Component in Tg (mpx:EGFP) Zebrafish and the Inhibitory Effects were Associated with the Regulation of Inflammation-Related Genes. It has been known that excessive and uncontrolled inflammation can cause various chronic inflam-

https://doi.org/10.1021/acsomega.3c04281
ACS Omega 2023, 8, 40260−40276

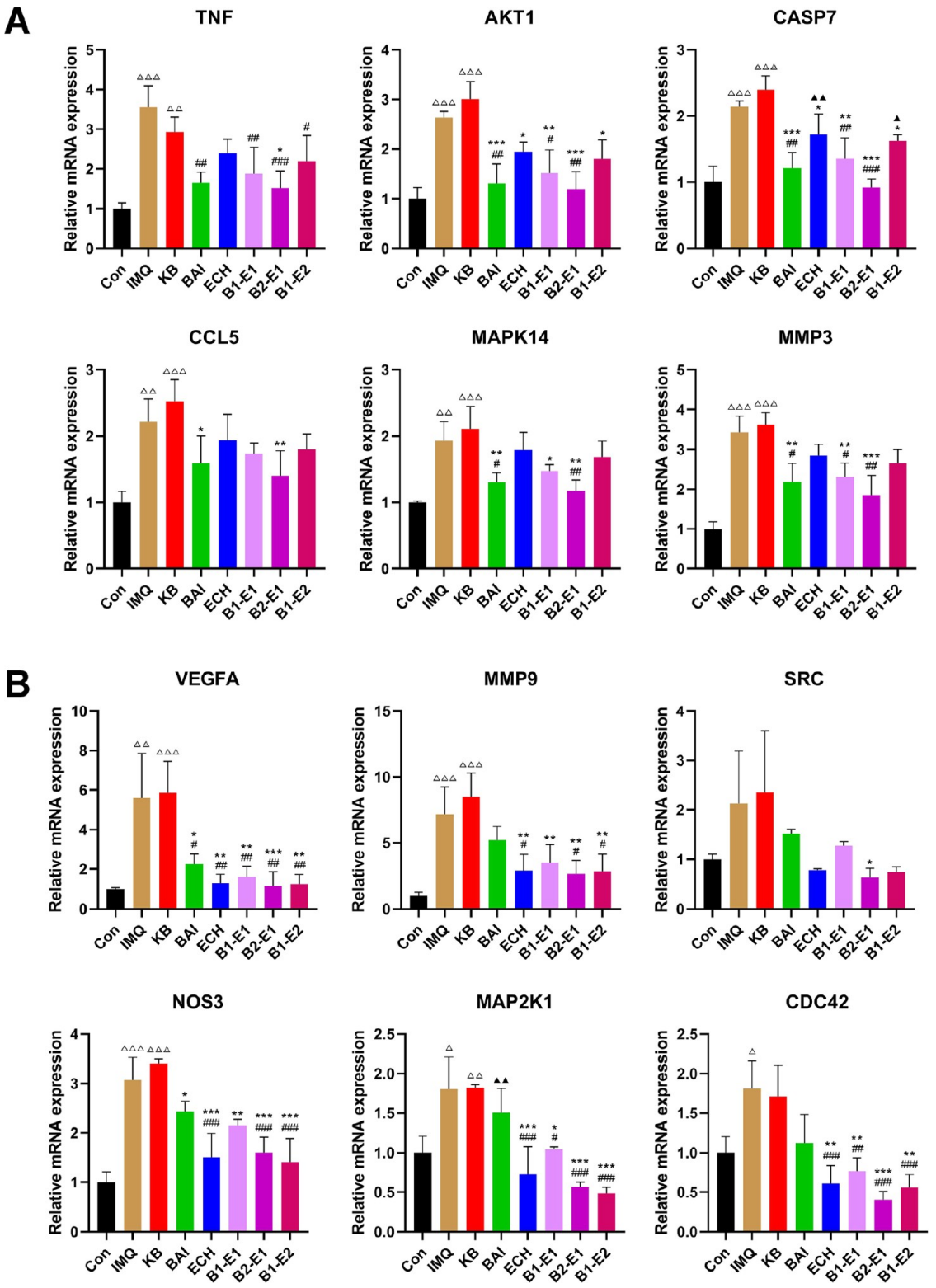

Figure 8. B2-E1 (BAI/ECH = 2:1) could notably regulate the mRNA expression of key genes in the TNF signaling pathway and the VEGF signaling pathway better than the single component in IMQ-induced mice. (A) B2-E1 could potently inhibit the mRNA expression of these genes related to key targets involved in the TNF signaling pathway better than the single component in IMQ-induced skin lesions (n = 6). (B) B2-E1 could significantly decrease the mRNA expression of these genes related to key targets involved in the VEGF signaling pathway better than the single component in IMQ-induced skin lesions (n = 6). Data are expressed as mean ± SD $^{\triangle}P < 0.05$, $^{\triangle\triangle}P < 0.01$, and $^{\triangle\triangle\triangle}P < 0.001$ versus the Con group, $^{\#}P < 0.05$ and $^{\#\#}P < 0.01$ and $^{\#\#\#}P < 0.001$ versus the IMQ group, $^{*}P < 0.05$, $^{**}P < 0.01$, and $^{***}P < 0.001$ versus the KB group, and $^{\blacktriangle}P < 0.05$ and $^{\blacktriangle\blacktriangle}P < 0.01$ versus the B2-E1 group.

matory diseases such as psoriasis, rheumatoid arthritis, and inflammatory bowel disease.[59] The inflammatory process is mediated by diverse inflammatory cells, including neutrophils, macrophages, eosinophils, and mononuclear phagocytes.[60] In

https://doi.org/10.1021/acsomega.3c04281
ACS Omega 2023, 8, 40260−40276

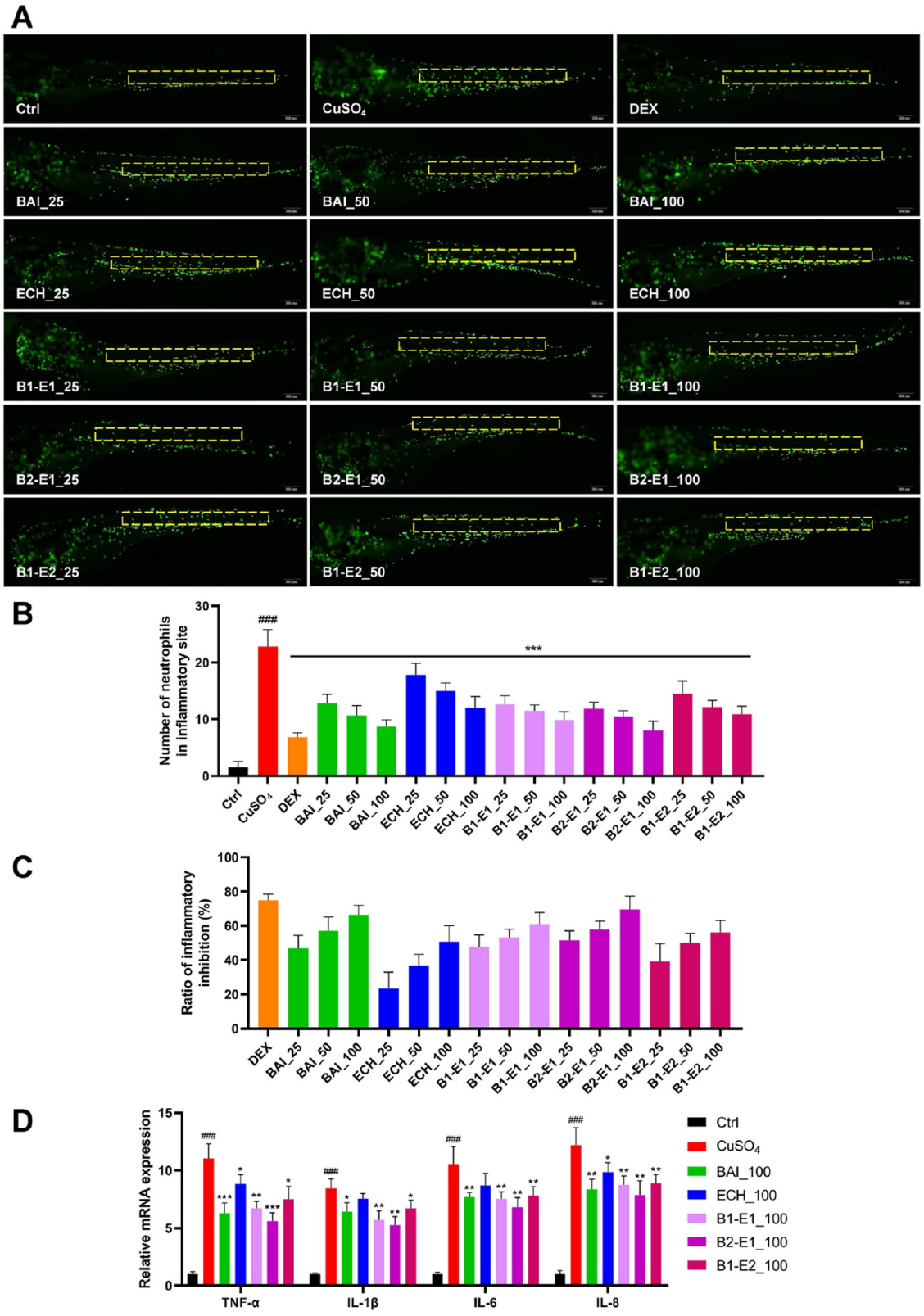

Figure 9. B2-E1 (BAI/ECH = 2:1) inhibited $CuSO_4$-induced neutrophils migration better than the single component in Tg (mpx:EGFP) zebrafish, and the inhibitory effects were associated with inhibiting the mRNA expression of inflammation-related genes. (A) Representative microphotographs of neutrophil migration in Tg (mpx:EGFP) zebrafish larvae in each group (neutrophils of 3 dpf Tg (mpx:EGFP) zebrafish larvae exhibiting green fluorescence; n = 10). The boxed region with dotted yellow lines indicates the recruitment of neutrophils to the inflammatory site of zebrafish larvae. (B) The number of neutrophils recruited in the inflammatory site (n = 10). (C) The ratio of inflammatory inhibition (n = 10). (D) Relative mRNA expression of inflammation-related genes including TNF-α, IL-1β, IL-6, and IL-8 in each group (n = 20). Data are represented as mean ± SD $^{\#\#\#}P < 0.001$ versus the Ctrl group and $^{*}P < 0.05$, $^{**}P < 0.01$, and $^{***}P < 0.001$ versus the $CuSO_4$ group.

https://doi.org/10.1021/acsomega.3c04281
ACS Omega 2023, 8, 40260−40276

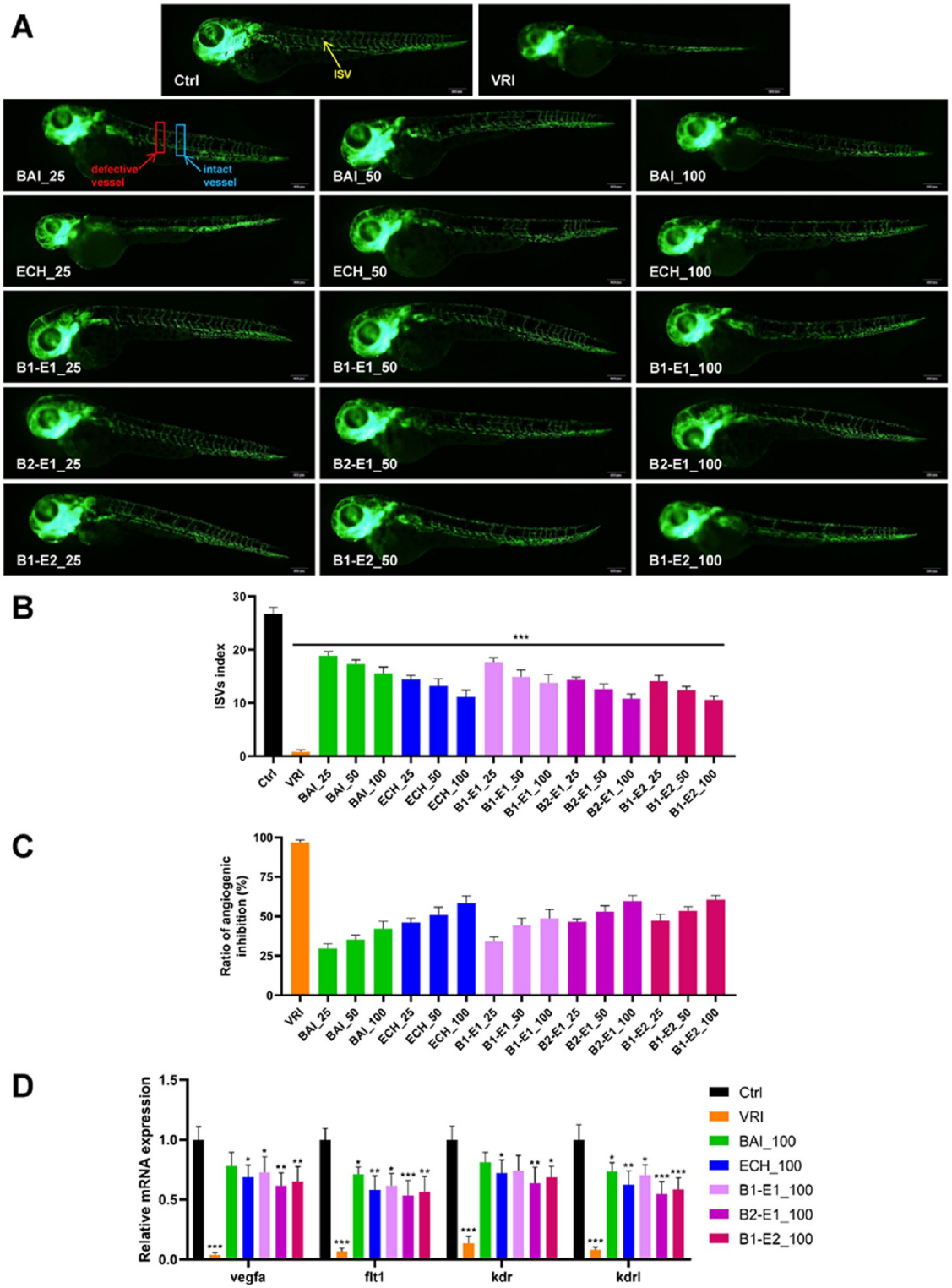

Figure 10. B2-E1 (BAI/ECH = 2:1) inhibited angiogenesis better than the single component in Tg (fli1:EGFP) zebrafish, and the inhibitory effects were associated with inhibiting the mRNA expression of angiogenesis-related genes. (A) Representative microphotographs of angiogenesis in Tg (fli1:EGFP) zebrafish larvae in each group (vascular endothelial cells of 48 hpf Tg (fli1:EGFP) zebrafish larvae exhibiting green fluorescence; n = 10). The yellow arrow indicated the intersegmental blood vessel (ISV) of zebrafish larvae. Red and light blue arrows indicated the defective ISV and intact ISV of zebrafish larvae, respectively. (B) Statistical analysis of ISVs index in each group (n = 10). (C) The ratio of angiogenic inhibition in each group (n = 10). (D) Relative mRNA expression of angiogenesis-related genes including vegfa, flt1, kdr, and kdrl in each group (n = 20). Data are expressed as mean ± SD. $^{*}P < 0.05$, $^{**}P < 0.01$, and $^{***}P < 0.001$ versus the Ctrl group.

particular, excessive recruitment and uncontrolled migration of neutrophils to injured sites can result in tissue damage and disease.[61] To evaluate the anti-inflammatory effect of BAI or ECH or BAI combined with ECH in detail, the inflammatory cell accumulation was tested in Tg (mpx:EGFP) zebrafish larvae. It was used to observe the migration of neutrophils

https://doi.org/10.1021/acsomega.3c04281
ACS Omega 2023, 8, 40260−40276

labeled with green fluorescence, indicating that the marked neutrophils have the ability to migrate to the inflammatory site.[62] In this experiment, drug treatment groups were separately treated with DEX, BAI, ECH, B1-E1, B2-E1, and B1-E2 for 6 h after exposure to $CuSO_4$ for 2 h. As shown in Figure 9A, neutrophils migrated significantly to the inflammatory site of Tg (mpx:EGFP) zebrafish larvae in the $CuSO_4$ group compared to the Ctrl group. Meanwhile, drug treatment groups could decrease the trend of recruitment of neutrophils. In addition, the number of neutrophils in the inflammatory site (Figure 9B) and the ratio of inflammatory inhibition (Figure 9C) were further analyzed. The results showed the significant inhibitory effect of drug treatment groups on neutrophil recruitment to the inflammatory site ($P < 0.001$), particularly the better effect of B2-E1 than those of the single component, B1-E1, and B1-E2.

Previous studies have indicated that TNF-α, IL-1β, IL-6, and IL-8 are crucial proinflammatory factors that play key roles in inflammation and autoimmunization.[63] To reveal the potential anti-inflammatory mechanism of BAI combined with ECH, the mRNA expression of inflammation-related genes (TNF-α, IL-1β, IL-6, and IL-8) in each group was then measured by qPCR. As shown in Figure 9D, the relative mRNA expression of TNF-α, IL-1β, IL-6, and IL-8 was significantly increased in the $CuSO_4$ group compared to that in the Ctrl group ($P < 0.001$). Compared with the $CuSO_4$ group, BAI combined with ECH could inhibit the mRNA expression of TNF-α, IL-1β, IL-6, and IL-8 to a certain degree ($P < 0.05$, $P < 0.01$, $P < 0.001$), especially the better effect of B2-E1 than those of the single component, B1-E1, and B1-E2.

3.5. B2-E1 Inhibited Angiogenesis Better than the Single Component in Tg (fli1:EGFP) Zebrafish and the Inhibitory Effects were Associated with the Regulation of Angiogenesis-Related Genes. It has been reported that abnormal angiogenesis or pathological angiogenesis is associated with the development of inflammatory diseases, including cancer, psoriasis, and rheumatoid arthritis.[64] It has suggested that inflammation and angiogenesis are codependent.[65] Thus, targeting angiogenesis is a potential therapeutic strategy in the treatment of chronic inflammation.[65] To assess the antiangiogenic effect of BAI or ECH or BAI combined with ECH specifically, Tg (fli1:EGFP) zebrafish was then used in this study. Due to the vessels labeled with green fluorescence in Tg (fli1:EGFP) zebrafish, the phenotype of angiogenesis can be observed directly.[66] In this experiment, drug treatment groups were separately treated with VRI, BAI, ECH, B1-E1, B2-E1, and B1-E2 for 24 h. As shown in Figure 10A−C, the angiogenesis was significantly inhibited in drug treatment groups compared to the Ctrl group ($P < 0.001$), particularly the better effect of ECH, B2-E1, and B1-E2 than those of BAI and B1-E1.

Previous studies have indicated that the VEGF signaling pathway plays an important role in the regulation of angiogenesis, and it is also well studied in the angiogenesis of zebrafish.[67,68] VEGF (vegfa) is the mostly studied growth factor for the vasculature development of zebrafish.[69] VEGFR-1 (flt1) and VEGFR-2 (kdr and kdrl), mainly expressed in vascular endothelial cells, also encode VEGF receptors in zebrafish.[70] To illustrate the potential antiangiogenic mechanism of BAI combined with ECH, the mRNA expression of angiogenesis-related genes (vegfa, flt1, kdr, and kdrl) in each group was then measured by qPCR. As shown in Figure 10D, the relative mRNA expression of vegfa, flt1, kdr, and kdrl was significantly decreased in VRI, ECH, B2-E1, and B1-E2 groups compared to the Ctrl group ($P < 0.05$, $P < 0.01$, $P < 0.001$).

4. CONCLUSIONS

Topical application of BAI combined with ECH could ameliorate IMQ-induced skin lesions, particularly the better effects of B2-E1. Furthermore, the significant effects were associated with inhibiting the expression of key cytokines and genes such as TNF-α, IL-17A, IL-23, and AKT1 by regulating the TNF signaling pathway and suppressing the expression of key cytokines and genes such as VEGFA, MMP9, SRC, and NOS3 by regulating the VEGF signaling pathway (Figure 11).

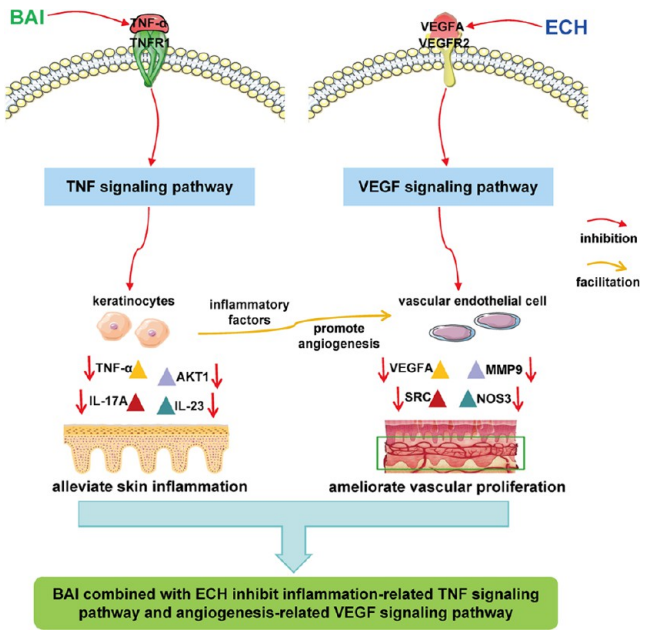

Figure 11. Potential mechanism of topical application of BAI combined with ECH ameliorating psoriatic skin lesions by inhibiting the TNF signaling pathway and the VEGF signaling pathway. BAI may inhibit the expression of key cytokines and genes such as TNF-α, IL-17A, IL-23, and AKT1 by regulating the TNF signaling pathway, and ECH could inhibit the expression of key cytokines and genes such as VEGFA, MMP9, SRC, and NOS3 by regulating the VEGF signaling pathway.

Meanwhile, zebrafish experiments further demonstrated the anti-inflammatory and antiangiogenic effects of BAI combined with ECH by regulating the inflammation-related TNF signaling pathway and the angiogenesis-related VEGF signaling pathway. Thus, this study suggested that BAI combined with ECH may be a promising topical agent to ameliorate psoriatic skin lesions by regulating the TNF signaling pathway and the VEGF signaling pathway in the future.

■ ASSOCIATED CONTENT

Data Availability Statement

All data are available on request.

Supporting Information

The Supporting Information is available free of charge at https://pubs.acs.org/doi/10.1021/acsomega.3c04281.

Optimization of the cream preparation by the multifactor orthogonal test; PCR primers used in this study; and prediction of potential targets and pathways of BAI

https://doi.org/10.1021/acsomega.3c04281
ACS Omega 2023, 8, 40260−40276

treating PSO and ECH treating PSO on the skin by network pharmacology and molecular docking (PDF)

AUTHOR INFORMATION

Corresponding Author

Xinyu Li − *Institute of Dermatology, Chinese Academy of Medical Sciences and Peking Union Medical College, Nanjing 210042, China*; orcid.org/0000-0003-2217-0548; Email: xinyusli609@163.com

Authors

Yi Chen − *Institute of Dermatology, Chinese Academy of Medical Sciences and Peking Union Medical College, Nanjing 210042, China*

Yongfang Wang − *Institute of Dermatology, Chinese Academy of Medical Sciences and Peking Union Medical College, Nanjing 210042, China*

Shasha Song − *Institute of Dermatology, Chinese Academy of Medical Sciences and Peking Union Medical College, Nanjing 210042, China*

Xiaoli Zhang − *Institute of Dermatology, Chinese Academy of Medical Sciences and Peking Union Medical College, Nanjing 210042, China*

Lili Wu − *Institute of Dermatology, Chinese Academy of Medical Sciences and Peking Union Medical College, Nanjing 210042, China*

Jianbing Wu − *Institute of Dermatology, Chinese Academy of Medical Sciences and Peking Union Medical College, Nanjing 210042, China*

Complete contact information is available at: https://pubs.acs.org/10.1021/acsomega.3c04281

Author Contributions

X.L. and Y.C. designed the study. Y.C., Y.W., S.S., X.Z., L.W., and J.W. performed the experiments. Y.C. processed the experimental data and analyzed the results. Y.C. drafted the first versions. X.L. contributed to text revision and discussion. All authors reviewed the manuscript and approved the final version.

Notes

The authors declare no competing financial interest.

ACKNOWLEDGMENTS

This work was supported by a grant from the Chinese Academy of Medical Sciences (CAMS) Innovation Fund for Medical Sciences (CAMS-2017-I2M-1-011).

REFERENCES

(1) Zhou, X.; Chen, Y.; Cui, L.; Shi, Y.; Guo, C. Advances in the pathogenesis of psoriasis: from keratinocyte perspective. *Cell Death Dis.* **2022**, *13*, 81.

(2) Elias, P. M.; Arbiser, J.; Brown, B. E.; Rossiter, H.; Man, M. Q.; Cerimele, F.; Crumrine, D.; Gunathilake, R.; Choi, E. H.; Uchida, Y.; Tschachler, E.; Feingold, K. R. Epidermal vascular endothelial growth factor production is required for permeability barrier homeostasis, dermal angiogenesis, and the development of epidermal hyperplasia: implications for the pathogenesis of psoriasis. *Am. J. Pathol.* **2008**, *173*, 689−699.

(3) Ru, Y.; Li, H.; Zhang, R.; Luo, Y.; Song, J.; Kuai, L.; Xing, M.; Hong, S.; Sun, X.; Ding, X.; Lu, Y.; Liu, L.; Na, C.; Zhou, Y.; Li, B.; Li, X. Role of keratinocytes and immune cells in the anti-inflammatory effects of *Tripterygium wilfordii* Hook. f. in a murine model of psoriasis. *Phytomedicine* **2020**, *77*, No. 153299.

(4) Yamanaka, K.; Yamamoto, O.; Honda, T. Pathophysiology of psoriasis: a review. *J. Dermatol.* **2021**, *48*, 722−731.

(5) Bos, J. D.; Spuls, P. I. Topical treatments in psoriasis: today and tomorrow. *Clin. Dermatol.* **2008**, *26*, 432−437.

(6) Oray, M.; Abu Samra, K.; Ebrahimiadib, N.; Meese, H.; Foster, C. S. Long-term side effects of glucocorticoids. *Expert Opin. Drug Saf.* **2016**, *15*, 457−465.

(7) Gendrisch, F.; Haarhaus, B.; Krieger, N.; Quirin, K. W.; Schempp, C. M.; Wölfle, U. The effect of herbal medicinal products on psoriasis-like keratinocytes. *Biomolecules* **2021**, *11*, 371.

(8) Dinda, B.; Dinda, S.; DasSharma, S.; Banik, R.; Chakraborty, A.; Dinda, M. Therapeutic potentials of baicalin and its aglycone, baicalein against inflammatory disorders. *Eur. J. Med. Chem.* **2017**, *131*, 68−80.

(9) Sowndhararajan, K.; Deepa, P.; Kim, M.; Park, S. J.; Kim, S. Neuroprotective and cognitive enhancement potentials of baicalin: a review. *Brain Sci.* **2018**, *8*, 104.

(10) Li-Weber, M. New therapeutic aspects of flavones: the anticancer properties of *Scutellaria* and its main active constituents Wogonin, Baicalein and Baicalin. *Cancer Treat. Rev.* **2009**, *35*, 57−68.

(11) Yang, J. Y.; Li, M.; Zhang, C. L.; Liu, D. Pharmacological properties of baicalin on liver diseases: a narrative review. *Pharmacol. Rep.* **2021**, *73*, 1230−1239.

(12) Kim, E.; Ham, S.; Jung, B. K.; Park, J. W.; Kim, J.; Lee, J. H. Effect of baicalin on wound healing in a mouse model of pressure ulcers. *Int. J. Mol. Sci.* **2023**, *24*, 329.

(13) Sherwani, M. A.; Yang, K.; Jani, A.; Abed, R. A.; Taufique, A. K.; Dosunmu, T. G.; Yusuf, N. Protective effect of baicalin against TLR4-mediated UVA-induced skin inflammation. *Photochem. Photobiol.* **2019**, *95*, 605−611.

(14) Xing, F.; Yi, W. J.; Miao, F.; Su, M. Y.; Lei, T. C. Baicalin increases hair follicle development by increasing canonical Wnt/β-catenin signaling and activating dermal papillar cells in mice. *Int. J. Mol. Med.* **2018**, *41*, 2079−2085.

(15) Burlou-Nagy, C.; Bănică, F.; Jurca, T.; Vicaş, L. G.; Marian, E.; Muresan, M. E.; Bácskay, I.; Kiss, R.; Fehér, P.; Pallag, A. *Echinacea purpurea* (L.) Moench: biological and pharmacological properties—A review. *Plants* **2022**, *11*, 1244.

(16) Liu, J.; Tang, N.; Liu, N.; Lei, P.; Wang, F. Echinacoside inhibits the proliferation, migration, invasion and angiogenesis of ovarian cancer cells through PI3K/AKT pathway. *J. Mol. Histol.* **2022**, *53*, 493−502.

(17) Wei, W.; Lan, X. B.; Liu, N.; Yang, J. M.; Du, J.; Ma, L.; Zhang, W. J.; Niu, J. G.; Sun, T.; Yu, J. Q. Echinacoside alleviates hypoxic-ischemic brain injury in neonatal rat by enhancing antioxidant capacity and inhibiting apoptosis. *Neurochem. Res.* **2019**, *44*, 1582−1592.

(18) Zhou, L.; Yao, M.; Tian, Z.; Song, Y.; Sun, Y.; Ye, J.; Li, G.; Sng, K. S.; Xu, L.; Cui, X.; Wang, Y. Echinacoside attenuates inflammatory response in a rat model of cervical spondylotic myelopathy via inhibition of excessive mitochondrial fission. *Free Radical Biol. Med.* **2020**, *152*, 697−714.

(19) Tang, C.; Gong, L.; Lvzi, X.; Qiu, K.; Zhang, Z.; Wan, L. Echinacoside inhibits breast cancer cells by suppressing the Wnt/β-catenin signaling pathway. *Biochem. Biophys. Res. Commun.* **2020**, *526*, 170−175.

(20) Zhang, D.; Lu, C.; Yu, Z.; Wang, X.; Yan, L.; Zhang, J.; Li, H.; Wang, J.; Wen, A. Echinacoside alleviates UVB irradiation-mediated skin damage via inhibition of oxidative stress, DNA damage, and apoptosis. *Oxid. Med. Cell. Longevity* **2017**, *2017*, No. 6851464.

(21) Sangaraju, R.; Alavala, S.; Nalban, N.; Jerald, M. K.; Sistla, R. Galangin ameliorates Imiquimod-Induced psoriasis-like skin inflammation in BALB/c mice via down regulating NF-κB and activation of Nrf2 signaling pathways. *Int. Immunopharmacol.* **2021**, *96*, No. 107754.

(22) Liu, X.; Yu, X.; Zack, D. J.; Zhu, H.; Qian, J. TiGER: a database for tissue-specific gene expression and regulation. *BMC Bioinf.* **2008**, *9*, 271.

(23) Zhou, H.; Cao, H.; Zheng, Y.; Lu, Z.; Chen, Y.; Liu, D.; Yang, H.; Quan, J.; Huo, C.; Liu, J.; Yu, L. Liang-Ge-San, a classic traditional Chinese medicine formula, attenuates acute inflammation in zebrafish and RAW 264.7 cells. *J. Ethnopharmacol.* **2020**, *249*, No. 112427.
(24) Wang, Y.; Tian, J.; Shi, F.; Li, X.; Hu, Z.; Chu, J. Protective effect of surfactin on copper sulfate-induced inflammation, oxidative stress, and hepatic injury in zebrafish. *Microbiol. Immunol.* **2021**, *65*, 410−421.
(25) Wang, Y.; Lu, J.; Qu, H.; Cai, C.; Liu, H.; Chu, J. β-Carotene extracted from *Blakeslea trispora* attenuates oxidative stress, inflammatory, hepatic injury and immune damage induced by copper sulfate in zebrafish (*Danio rerio*). *Comp. Biochem. Physiol. C* **2022**, *258*, No. 109366, DOI: 10.1016/j.cbpc.2022.109366.
(26) Alex, D.; Lam, I. K.; Lin, Z.; Lee, S. M. Indirubin shows anti-angiogenic activity in an *in vivo* zebrafish model and an *in vitro* HUVEC model. *J. Ethnopharmacol.* **2010**, *131*, 242−247.
(27) Chen, K.; Fan, Y.; Gu, J.; Han, Z.; Zeng, H.; Mao, C.; Wang, C. In vivo screening of natural products against angiogenesis and mechanisms of anti-angiogenic activity of deoxysappanone B 7,4′-dimethyl ether. *Drug Des. Dev. Ther.* **2020**, *14*, 3069−3078.
(28) Isogai, S.; Lawson, N. D.; Torrealday, S.; Horiguchi, M.; Weinstein, B. M. Angiogenic network formation in the developing vertebrate trunk. *Development* **2003**, *130*, 5281−5290.
(29) Chen, Y.; Chen, P. D.; Bao, B. H.; Shan, M. Q.; Zhang, K. C.; Cheng, F. F.; Cao, Y. D.; Zhang, L.; Ding, A. W. Anti-thrombotic and pro-angiogenic effects of *Rubia cordifolia* extract in zebrafish. *J. Ethnopharmacol.* **2018**, *219*, 152−160.
(30) Fantuzzi, F.; Del Giglio, M.; Gisondi, P.; Girolomoni, G. Targeting tumor necrosis factor alpha in psoriasis and psoriatic arthritis. *Expert Opin. Ther. Targets* **2008**, *12*, 1085−1096.
(31) Renzo, L. D.; Saraceno, R.; Schipani, C.; Rizzo, M.; Bianchi, A.; Noce, A.; Esposito, M.; Tiberti, S.; Chimenti, S.; DE Lorenzo, A. Prospective assessment of body weight and body composition changes in patients with psoriasis receiving anti-TNF-α treatment. *Dermatol. Ther.* **2011**, *24*, 446−451.
(32) Li, J.; Hou, H.; Zhou, L.; Wang, J.; Liang, J.; Li, J.; Hou, R.; Niu, X.; Yin, G.; Li, X.; Zhang, K. Increased angiogenesis and migration of dermal microvascular endothelial cells from patients with psoriasis. *Exp. Dermatol.* **2021**, *30*, 973−981.
(33) Micali, G.; Lacarrubba, F.; Musumeci, M. L.; Massimino, D.; Nasca, M. R. Cutaneous vascular patterns in psoriasis. *Int. J. Dermatol.* **2010**, *49*, 249−256.
(34) Ahmad, A.; Nawaz, M. I. Molecular mechanism of VEGF and its role in pathological angiogenesis. *J. Cell. Biochem.* **2022**, *123*, 1938−1965.
(35) Benhadou, F.; Glitzner, E.; Brisebarre, A.; Swedlund, B.; Song, Y.; Dubois, C.; Rozzi, M.; Paulissen, C.; Del Marmol, V.; Sibilia, M.; Blanpain, C. Epidermal autonomous VEGFA/Flt1/Nrp1 functions mediate psoriasis-like disease. *Sci. Adv.* **2020**, *6*, No. eaax5849.
(36) Ozma, M. A.; Khodadadi, E.; Pakdel, F.; Kamounah, F. S.; Yousefi, M.; Yousefi, B.; Asgharzadeh, M.; Ganbarov, K.; Kafil, H. S. Baicalin, a natural antimicrobial and anti-biofilm agent. *J. Herb. Med.* **2021**, *27*, No. 100432.
(37) Kim, Y. W.; West, X. Z.; Byzova, T. V. Inflammation and oxidative stress in angiogenesis and vascular disease. *J. Mol. Med.* **2013**, *91*, 323−328.
(38) West, X. Z.; Malinin, N. L.; Merkulova, A. A.; Tischenko, M.; Kerr, B. A.; Borden, E. C.; Podrez, E. A.; Salomon, R. G.; Byzova, T. V. Oxidative stress induces angiogenesis by activating TLR2 with novel endogenous ligands. *Nature* **2010**, *467*, 972−976.
(39) Zhou, Q.; Mrowietz, U.; Rostami-Yazdi, M. Oxidative stress in the pathogenesis of psoriasis. *Free Radical Biol. Med.* **2009**, *47*, 891−905.
(40) Jang, D. I.; Lee, A. H.; Shin, H. Y.; Song, H. R.; Park, J. H.; Kang, T. B.; Lee, S. R.; Yang, S. H. The role of tumor necrosis factor alpha (TNF-α) in autoimmune disease and current TNF-α inhibitors in therapeutics. *Int. J. Mol. Sci.* **2021**, *22*, 2719.
(41) Nadeem, A.; Al-Harbi, N. O.; Al-Harbi, M. M.; El-Sherbeeny, A. M.; Ahmad, S. F.; Siddiqui, N.; Al-Sharary, S. D.; et al. Imiquimod-induced psoriasis-like skin inflammation is suppressed by BET bromodomain inhibitor in mice through RORC/IL-17A pathway modulation. *Pharmacol. Res.* **2015**, *99*, 248−257.
(42) Wang, A. O.; Bai, Y. Dendritic cells: The driver of psoriasis. *J. Dermatol.* **2020**, *47*, 104−113.
(43) Ogawa, E.; Sato, Y.; Minagawa, A.; Okuyama, R. Pathogenesis of psoriasis and development of treatment. *J. Dermatol.* **2018**, *45*, 264−272.
(44) Armstrong, A. W.; Read, C. Pathophysiology, clinical presentation, and treatment of psoriasis: A review. *JAMA* **2020**, *323*, 1945−1960.
(45) Kobayashi, K.; Chikazawa, S.; Chen, Y.; Suzuki, S.; Ichimasu, N.; Katagiri, K. Oestrogen inhibits psoriasis-like dermatitis induced by imiquimod in mice in relation to increased IL-10 producing cells despite elevated expression of IL-22, IL-23, IL-17 mRNA. *Exp. Dermatol.* **2023**, *32*, 203−209.
(46) Abhinand, C. S.; Raju, R.; Soumya, S. J.; Arya, P. S.; Sudhakaran, P. R. VEGF-A/VEGFR2 signaling network in endothelial cells relevant to angiogenesis. *J. Cell Commun. Signal.* **2016**, *10*, 347−354.
(47) Hawinkels, L. J.; Zuidwijk, K.; Verspaget, H. W.; de Jonge-Muller, E. S.; van Duijn, W.; Ferreira, V.; Fontijn, R. D.; David, G.; Hommes, D. W.; Lamers, C. B.; Sier, C. F. VEGF release by MMP-9 mediated heparan sulphate cleavage induces colorectal cancer angiogenesis. *Eur. J. Cancer* **2008**, *44*, 1904−1913.
(48) Radomska-Leśniewska, D. M.; Bałan, B. J.; Skopiński, P. Angiogenesis modulation by exogenous antioxidants. *Cent. Eur. J. Immunol.* **2017**, *42*, 370−376.
(49) Schuerwegh, A. J.; Dombrecht, E. J.; Stevens, W. J.; Van Offel, J. F.; Bridts, C. H.; De Clerck, L. S. Influence of pro-inflammatory (IL-1 alpha, IL-6, TNF-alpha, IFN-gamma) and anti-inflammatory (IL-4) cytokines on chondrocyte function. *Osteoarthritis Cartilage* **2003**, *11*, 681−687.
(50) Li, Y.; Zou, L.; Li, T.; Lai, D.; Wu, Y.; Qin, S. Mogroside V inhibits LPS-induced COX-2 expression/ROS production and overexpression of HO-1 by blocking phosphorylation of AKT1 in RAW264.7 cells. *Acta Biochem. Biophys. Sin.* **2019**, *51*, 365−374.
(51) Marques, R. E.; Guabiraba, R.; Russo, R. C.; Teixeira, M. M. Targeting CCL5 in inflammation. *Expert Opin. Ther. Targets* **2013**, *17*, 1439−1460.
(52) Kan, H.; Wang, Y.; Wang, D.; Sun, H.; Zhou, S.; Wang, H.; Guan, J.; Li, M. Cordycepin rescues lidocaine-induced neurotoxicity in dorsal root ganglion by interacting with inflammatory signaling pathway MMP3. *Eur. J. Pharmacol.* **2018**, *827*, 88−93.
(53) Shang, Z.; Lv, H.; Zhang, M.; Duan, L.; Wang, S.; Li, J.; Liu, G.; Ruijie, Z.; Jiang, Y. Genome-wide haplotype association study identify TNFRSF1A, CASP7, LRP1B, CDH1 and TG genes associated with Alzheimer's disease in Caribbean Hispanic individuals. *Oncotarget* **2015**, *6*, 42504−42514.
(54) Ali, E. M. H.; Abdel-Maksoud, M. S.; Hassan, R. M.; Mersal, K. I.; Ammar, U. M.; Se-In, C.; He-Soo, H.; Kim, H. K.; Lee, A.; Lee, K. T.; Oh, C. H. Design, synthesis and anti-inflammatory activity of imidazol-5-yl pyridine derivatives as p38α/MAPK14 inhibitor. *Bioorg. Med. Chem.* **2021**, *31*, No. 115969.
(55) Schlessinger, J. New roles for Src kinases in control of cell survival and angiogenesis. *Cell* **2000**, *100*, 293−296.
(56) Saleh, A.; Stathopoulou, M. G.; Dadé, S.; Ndiaye, N. C.; Azimi-Nezhad, M.; Murray, H.; Masson, C.; Lamont, J.; Fitzgerald, P.; Visvikis-Siest, S. Angiogenesis related genes NOS3, CD14, MMP3 and IL4R are associated to VEGF gene expression and circulating levels in healthy adults. *BMC Med. Genet.* **2015**, *16*, 90.
(57) Xu, Q.; Liu, Z.; Zhu, Z. Q.; Fan, Y.; Chen, R.; Xie, X. H.; Cheng, M. Knockdown of growth factor receptor bound protein 7 suppresses angiogenesis by inhibiting the secretion of vascular endothelial growth factor A in ovarian cancer cells. *Bioengineered* **2021**, *12*, 12179−12190.
(58) Yoshida, Y.; Yamada, A.; Akimoto, Y.; Abe, K.; Matsubara, S.; Hayakawa, J.; Tanaka, J.; Kinoshita, M.; Kato, T.; Ogata, H.; Sakashita, A.; Mishima, K.; Kubota, Y.; Kawakami, H.; Kamijo, R.;

Iijima, T. Cdc42 has important roles in postnatal angiogenesis and vasculature formation. *Dev. Biol.* **2021**, *477*, 64−69.
(59) Schett, G.; Neurath, M. F. Resolution of chronic inflammatory disease: universal and tissue-specific concepts. *Nat. Commun.* **2018**, *9*, No. 3261.
(60) Bhattacharya, K.; Andón, F. T.; El-Sayed, R.; Fadeel, B. Mechanisms of carbon nanotube-induced toxicity: focus on pulmonary inflammation. *Adv. Drug Delivery Rev.* **2013**, *65*, 2087−2097.
(61) Wang, X.; Robertson, A. L.; Li, J.; Chai, R. J.; Haishan, W.; Sadiku, P.; Ogryzko, N. V.; Everett, M.; Yoganathan, K.; Luo, H. R.; Renshaw, S. A.; Ingham, P. W. Inhibitors of neutrophil recruitment identified using transgenic zebrafish to screen a natural product library. *Dis. Model. Mech.* **2014**, *7*, 163−169, DOI: 10.1242/dmm.012047.
(62) Gong, L.; Yu, L.; Gong, X.; Wang, C.; Hu, N.; Dai, X.; Peng, C.; Li, Y. Exploration of anti-inflammatory mechanism of forsythiaside A and forsythiaside B in $CuSO_4$-induced inflammation in zebrafish by metabolomic and proteomic analyses. *J. Neuroinflamm.* **2020**, *17*, 173.
(63) Kleine, T. O.; Zwerenz, P.; Graser, C.; Zöfel, P. Approach to discriminate subgroups in multiple sclerosis with cerebrospinal fluid (CSF) basic inflammation indices and TNF-α, IL-1β, IL-6, IL-8. *Brain Res. Bull.* **2003**, *61*, 327−346.
(64) Carmeliet, P.; Jain, R. K. Angiogenesis in cancer and other diseases. *Nature* **2000**, *407*, 249−257.
(65) Jackson, J. R.; Seed, M. P.; Kircher, C. H.; Willoughby, D. A.; Winkler, J. D. The codependence of angiogenesis and chronic inflammation. *FASEB J.* **1997**, *11*, 457−465.
(66) Gawrońska-Grzywacz, M.; Piątkowska-Chmiel, I.; Popiołek, Ł.; Herbet, M.; Dudka, J. The N-Substituted-4-Methylbenzenesulphonyl Hydrazone inhibits angiogenesis in zebrafish Tg(fli1: EGFP) model. *Pharmaceuticals* **2022**, *15*, 1308.
(67) Basu, S.; Sachidanandan, C. Zebrafish: a multifaceted tool for chemical biologists. *Chem. Rev.* **2013**, *113*, 7952−7980.
(68) Cannon, J. E.; Upton, P. D.; Smith, J. C.; Morrell, N. W. Intersegmental vessel formation in zebrafish: requirement for VEGF but not BMP signalling revealed by selective and non-selective BMP antagonists. *Br. J. Pharmacol.* **2010**, *161*, 140−149.
(69) Koenig, A. L.; Baltrunaite, K.; Bower, N. I.; Rossi, A.; Stainier, D. Y.; Hogan, B. M.; Sumanas, S. Vegfa signaling promotes zebrafish intestinal vasculature development through endothelial cell migration from the posterior cardinal vein. *Dev. Biol.* **2016**, *411*, 115−127.
(70) Goishi, K.; Klagsbrun, M. Vascular endothelial growth factor and its receptors in embryonic zebrafish blood vessel development. *Curr. Top. Dev. Biol.* **2004**, *62*, 127−152.

https://doi.org/10.1021/acsomega.3c04281
ACS Omega 2023, 8, 40260−40276